CYCLO-STATIONARY ANALYSIS OF MODULATED SIGNALS USED IN COMMUNICATION SATELLITES FOR PROSPECTIVE SPECTRUM SENSING APPLICATION IN SATELLITE COGNITIVE RADIO

Submitted by:

Syed Shabeeh Ul Husnain

NUST201260523MPNEC45312F

Supervisor:

Dr. Bilal Muhammad Khan

Co-Supervisor:

Dr. Khawaja Bilal Ahmed Mahmood

THESIS

Submitted to:

Department of Electronic and Power Engineering

Pakistan Navy Engineering College Karachi

National University of Science and Technology, Islamabad Pakistan

In fulfilment of requirement for the award of the degree of

MASTER OF SCIENCE IN ELECTRICAL ENGINEERING

With Specialization in Communication Engineering


بسم الله الرحمن الرحيم

Table of Contents

List of Figures

List of Tables

List of Acronyms

ANN (ARTIFICIAL NEURAL NETWORKS)

BPSK (BINARY PHASE SHIFT KEYING)

CAF (CYCLIC AUTOCORRELATION FUNCTION)

CDP (CYCLIC DOMAIN PROFILE)

CR (COGNITIVE RADIO)

CSD (CYCLIC SPECTRAL DENSITY)

DFT (DISCRETE FOURIER TRANSFORM)

FAM (FFT ACCUMULATION METHOD)

FFT (FAST FOURIER TRANSFORM)

FPGA (FIELD PROGRAMMABLE GATE ARRAY)

GRC (GNURADIO COMPANION)

HOS (HIGHER ORDER STATISTICS)

I (INPHASE)

IF (INTERMEDIATE FREQUENCY)

IFT (INVERSE FOURIER TRANSFORM)

LNB (LOW NOISE BLOCK)

OFDM (ORTHOGONAL FREQUENCY DIVISION MULTIPLEXING)

PSD (POWER SPECTRAL DENSITY)

Q (QUADRATURE)

QPSK (QUADRATURE PHASE SHIFT KEYING)

QAM (QUADRATURE AMPLITUDE MODULATION)

SCF (SPECTRAL CORRELATION DENSITY)

SDR (SOFTWARE DEFINED RADIO)

SNR (SIGNAL TO NOISE RATIO)

SOF (SPECTRAL COHERENCE FUNCTION)

SCSD (SUM OF THE MAGNITUDE SQUARE OF THE CYCLIC SPECTRAL DENSITY)

USRP2 (UNIVERSAL SOFTWARE RADIO PERIPHERAL 2)

Abstract

The modulated signals used in the communication systems typically exhibits cyclic periodicity. It is due to the fact of using sinusoidal product modulators, use of repeating preambles, coding and multiplexing in modern communication. This property of signals can be analysed using cyclo-stationary analysis and based on that detection of a signal is possible. Spectral correlation function (SCF) of cyclic auto-correlation (CAF) has unique features for different modulated signals and noise. Different techniques are applied to SCF for extracting the features on the basis of which decision of detecting a signal or noise is made.

In this research, different modulated signals used in satellite communication are analysed using SCF. A signal detection technique is devised on the basis of utilizing unique feature exhibit by a normalized vector calculated on SCF along frequency axis. The devised technique identifies the presence of a signal or noise in the analysed data within the defined threshold set for detection. A very high resolution SCF calculation is also not required by the proposed technique which is significant in terms of fast processing. Further, cumulants are applied to the calculated vector which further classifies different modulations and noise distinctly.

The simulations are performed in MATLAB and to capture external world signals USRP2 is used.

Acknowledgement

I am very much grateful to Almighty ALLAH, the most merciful and beneficent, whose ample blessings enable us to recognize and pursue knowledge in life. My sincere gratitude to my supervisor Dr. Muhammad Bilal Khan, Assistant Professor, Department of Electronic and Power Engineering at PN Engineering College, NUST. I consider myself very lucky and honoured to have him as my supervisor. I thank him for his unprecedented attention and patience throughout the thesis work. I admire him as a teacher and as a person. I extend my thanks to Cdr. Dr. Attaullah Memon (PN) for his prompt help and suggestions to me as HoD of Post Graduate program.

In addition to above, I am also thankful to the guidance committee comprising of following faculty members who led me to achieve my target:

- Dr. Khawaja Bilal Ahmed Mahmood
- Cdr. Dr. Tariq Mairaj Rasool Khan
- Dr. Naeem Abbas

I want to take this opportunity to thank my family. Thank you for your prayers, love, encouragement and support. Thank you for everything.

Executive Summary

The research presented in this thesis utilizes the time smoothing method FFT accumulation method (FAM) [1], [10] for calculating the cyclic statistics of the real satellite signals and obtained SCF spectral correlation function (SCF) with low resolution frequency and cyclic frequency parameters. The main contributions are devising feature based less complex detection scheme by extracting feature vectors from the calculated SCF for signals and noise in the satellite spectrum. Resulting SCF for received satellite carriers and noise are presented. The proposed technique requires no prior information about the signal it is analysing within the sampled spectrum. There are also no specialized memory requirements as in [2], [17] or covariance matrix computations [13] making it reduced computationally complex [18]. USRP2 [22] is used to capture the signals which make the whole algorithm compatible to be used in a practical satellite cognitive radio. No pre-processing of the acquired samples is required for mitigating the satellite channel effects which ensures signal detection with lowest possible SNR in the satellite link. Further, cumulants are applied to the calculated vector used by the detection scheme. They are used to classify the type of modulation of the detected signal by the proposed detection technique. Successful ranges are obtained for BPSK, QPSK and 16-QAM carriers present in the satellite frequency band. A unique application of cumulants is thus obtained in the research. The computational complexity analysis of the whole detection and classification using cyclostationary analysis and application of cumulants on the feature vector shows that the proposed research leads towards a feasible spectrum sensing solution for satellite cognitive radios. The proposed research performs well with high probability of detection under low SNR conditions in the satellite channel.

Chapter 1. **Introduction**

1.1 Motivation

Satellite cognitive radios have been proposed in recent years, so that the static bandwidth of the satellite can be utilized by primary and secondary users. Cognitive radio needs spectrum sensing technique to sense the free radio channel for utilization. Cyclostationary analysis [2]-[4] is a hot research topic in the area of spectrum sensing because it is efficient than traditional energy detection analysis. Techniques based on this method are complex and computationally hungry [4] to be used in cognitive radios. Therefore, research in this area is still required. Special focus will be set to the modulated signals used in the communication satellites, since there is almost no or a very little research focusing this particular area [4]. If computational complexity of the detection technique is minimized, the research will help in developing algorithms for spectrum sensing modules for satellite cognitive radios.

1.2 Aims and Objectives

The aim of the proposed research is to devise a simpler technique for extracting feature from the SCF of the modulated signals used in communication satellites. The proposed technique of analysis should be working with low resolution parameters for spectral density calculation, so that it will be fast enough to be used in the cognitive radios for satellites as cyclostationary spectrum sensing algorithm.

1.3 Cyclostationary and Cognitive Radios for Satellite

Cyclostationary analysis of the modulated signals have been a vast topic of research for almost half a century [1], different aspects of this inherent property of modulated signals have been investigated in that period [1]. The main application of cyclostationarity of signals is in the domain of spectrum sensing as it has been a proven technique for this purpose than conventional energy detection [7]. After the advent of software defined radio (SDR) based cognitive radios (CRs) [3] to solve the problem of spectrum scarcity in the frequency bands, cyclostationary analysis have been adopted as a perfect choice for spectrum sensing [2]. The main focus in this context is in the terrestrial bands but their exploitation in satellite communication is still not explored [4]. Particularly, very few initiatives at academic and industrial level have addressed the spectrum sensing aspects for CR of satellite communication [4]. So, application of cyclostationary analysis to the modulated carriers in the satellite band is an open research area. The CR for satellite needs to detect the modulated carriers, while performing the spectrum sensing in order to provide opportunity spectrum

holes to the secondary users. There is a computational complexity associated with the cyclostationary based detection so the technique devised for satellite CR should be low in complexity with shorter number of samples and low resolution analysis [2].

In satellite communications, modulated carriers are generated with modems, function generators meant for this purpose and travels at around 36000 km up to the satellite transceiver [4]. The band pipe nature of the satellite sends them back to the downlink. So, this channel incorporated a lot of noisy effects in the communication signals and then intended CR should be working with these received signals having the effect of this long path channel. The importance of this scenario must be kept in mind, while designing the signal detection technique for satellite CR. In this research, properties of such signals are exploited and a simpler technique incorporating all the complexity parameters discussed above is being proposed for satellite CR. The platform for the design of practical CR is of great importance. This is due to the fact that if the designed algorithm for detection is not compatible with the CR platform, then the signal detection efficiency will be compromised. So, the USRP2 which has been a proven platform for practical SDR and CR development [22] is used to capture the satellite signals and the lab generated satellite signals. This will enable the developed algorithm to work as a practical spectrum sensing engine for a prospective satellite CR on a real CR platform as in [15]-[16], & [19]-[20].

1.4 Organization of Thesis Report

The thesis report is organized in the following chapters.

Chapter 1 is the introduction to cyclostationary and cognitive radios for satellite.

Chapter 2 is about the cyclostationary spectrum sensing techniques in literature.

Chapter 3 provides mathematical model of cyclostationary analysis using the FAM algorithm.

In **Chapter 4,** theoretical SCF of BPSK, QPSK & 16-QAM modulations are discussed.

In **Chapter 5,** proposed detection technique is discussed along with the applications of cumulants.

Chapter 6 has practical experimentation setup and measurement results.

Chapter 7 discusses and presents the simulation results. It also presents the comparative analysis of the proposed technique and other state-of-the-art techniques used for detection of the signals.

Chapter 8 provides performance analysis of the proposed spectrum sensing scheme.

Chapter 9 gives the conclusion and suggests the prospective future work.

A brief introduction of GNU radio and USRP2 (which are modern and the most developed open source SDR software and hardware platforms respectively) is presented in the following sections of the introduction.

1.5 GNU Radio Software

GNU Radio is an official project of GNU since 2001 [31], it is free with open source rights software. Its development toolkit has signal processing and operation blocks using which SDR systems can be implemented. These systems can be interfaced with available low-cost RF hardware or general purpose processors..GNU radio applications are based on python as the programming language. Main signal processing blocks in GNU radio are written in C^{++} programming language in processor having floating point arithmetic. In GNU radio signal processing blocks are built on C^{++} programming language, and they use python programming language as wrapper which connects together the signal processing block [31]. In Fig. 1-1 graphical user interface of GNU radio flow graph is shown. The application of GNU radio is known as GNU radio companion (GRC).

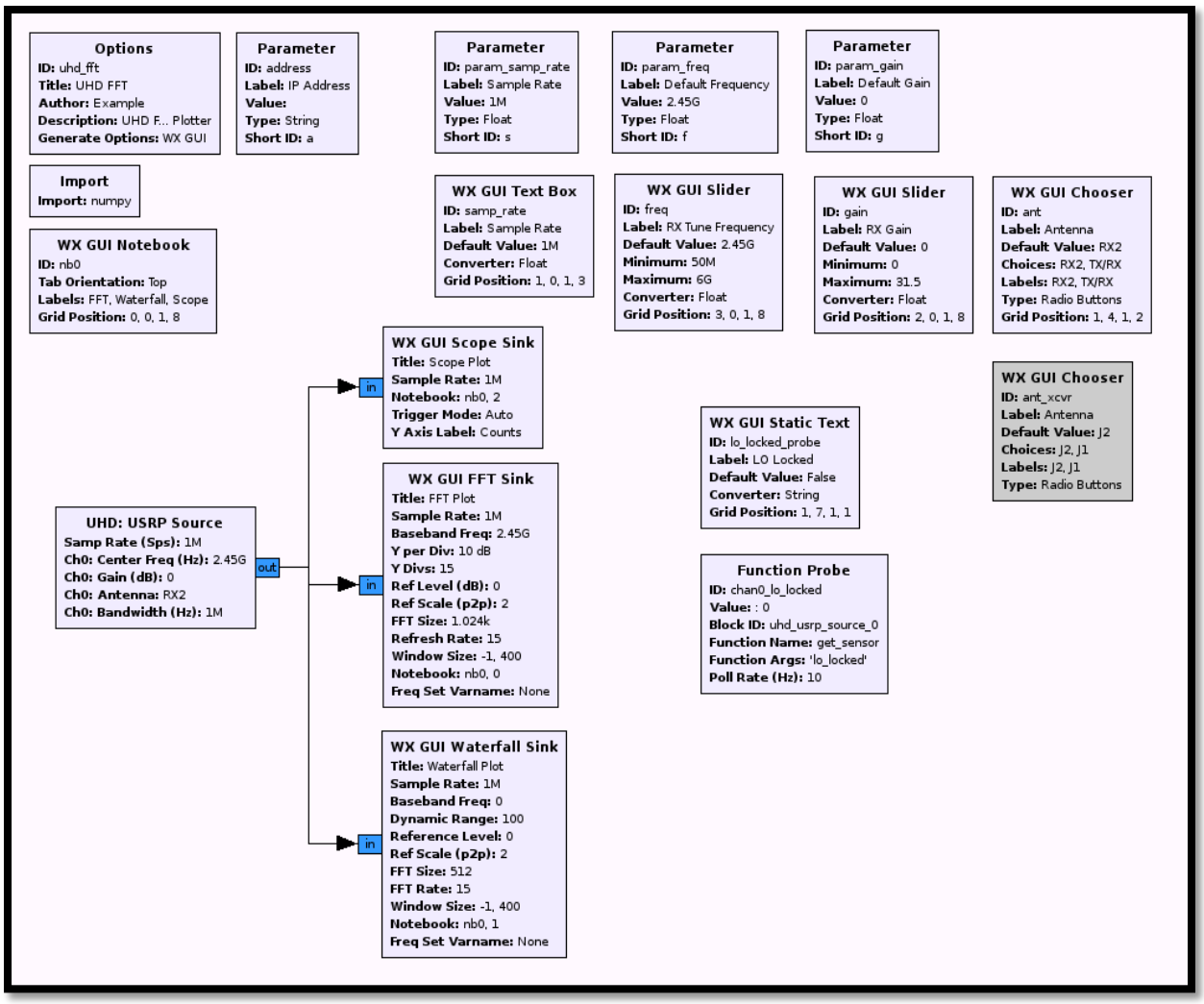

Figure 1-1: GUI of GNU radio flowgraph in GRC

1.6 USRP2

The universal software radio peripheral or USRP2 is a RF hardware front end sensor and pre processor used with GNU radio. It can convert normal computers into high bandwidth RF software radio instruments. Essentially, if a communication radio system is considered, USRP2 is the digital baseband and its daughter card is intermediate frequency (IF) equipments in the whole system. In a standard USRP2 two parts are included: (1) a mother board with a field-programmable gate array (FPGA), with high-speed processing feature for signals; (2) at-least one or more RF daughter boards designed to cover different bands of frequencies. The picture of USRP2 is present in Fig. 1-2 (a), and a picture of USRP2 mother board is present in Fig. 1-2 (b). The elements of USRP2 include a speedy 1Gbps Ethernet port which acts as the data bridge between PC and the FPGA, there are four 14bits/sample 100 Msamples/sec high-speed analog-to-digital convertors (ADCs) and four 16 bits/sample 400Msamples/sec high-speed digital-to-analog convertors (DACs). The mother board is

capable of supporting two transmit and receive daughter boards respectively. In order to change the operating frequency range we can choose different USRP2's daughter boards [29]. Examples are, wide-band transceiver (WBX) daughter board working at frequency range of 50-2200 MHz, RFX400 daughter board working at 400-500 MHz. In our experimentation, wide-band SBX transceiver with 400-4400 MHz range of frequency operation is used.

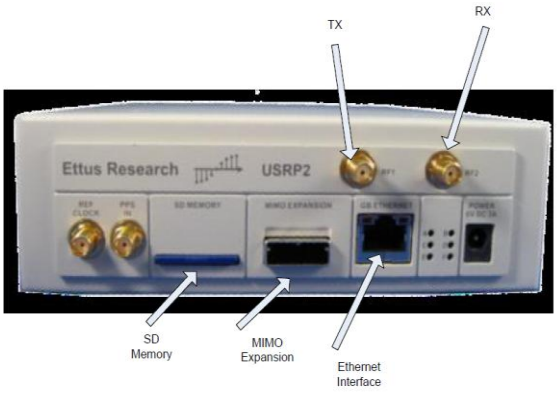

(a)

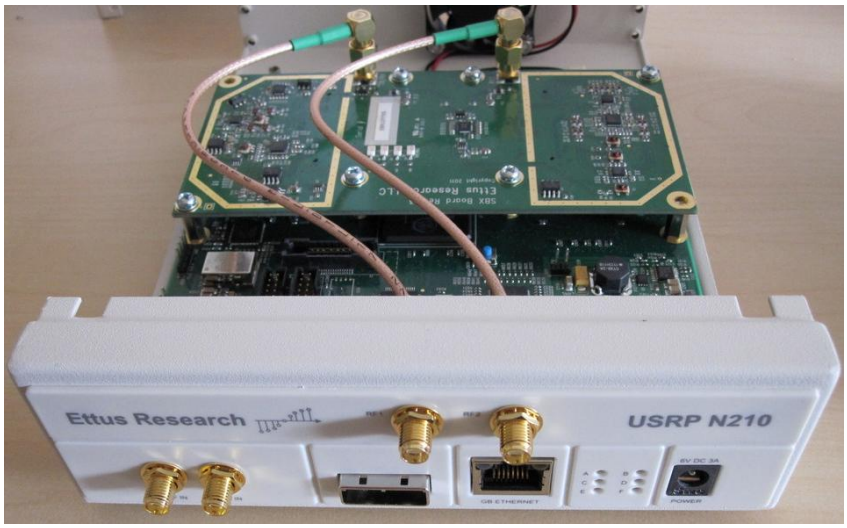

(b)

Figure 1-2 : (a) USRP2 front panel with interfaces (b) USRP2 mother board with SBX40 RF daughter cards

So far, an introductory idea has been presented. Modern SDR based CR development platform of GNU radio and hardware RF front-end of USRP2 is briefly discussed. In the following chapter, review of different cyclostationary based technique has been presented. Also, novel techniques for calculating the spectral density based on the correlation of cyclostationary modulated signals and their detection are going to be discussed.

Chapter 2. **Literature Review**

In this chapter, different approaches carried out in the literature for calculating the cyclostationary features of modulated signals are presented. The basic idea behind the approach, its significance, novelty and discrepancies are discussed. Specially, techniques using the second order statistics of the signal including the cyclic autocorrelation and the spectral correlation density for signal detection are focused.

2.1 Cyclostationary Detection

Cyclostationary for wireless signals that are present in signal processor is define by periodic variation in the statistical properties. These characteristics are time-varying with periodicity. For such wireless signals having periodicity property and modelled as cyclostationary signal, then functionality of signal processor can be enhanced by extracting cyclic features through signal detection based on features. Cyclostationary features shown by modulated carriers using signal processing of modulated sampled data is well developed in literature and has been used conventionally in wireless communication domain. The idea behind this special property of the signals is based on the fact that due to sine and cosine waves used to generate signals in a repeating manner so this introduces cyclic behaviour and a part from signal's carrier frequency there exists a frequency which is a function of repetition of the parameters of such waves. This frequency is called cyclic frequency. Cyclostationary theory as first introduced by Gardner [1] exploiting cyclo-periodic features of random processes opened new threads in wide research scope. Features exhibited by the random processes and modulated signals as a function of the frequency and cyclic frequency was discovered. Detailed analysis of the cyclic periodogram was presented. The autocorrelation which is a second order statistical property for a Guassian processes having normal distribution was used by the author. Spectral analysis of autocorrelation function led to the discovery of specific peaks in the spectral density at certain location of cyclic frequency as a function of the carrier frequency. This was the first time when a proper mathematical frame work for exploring the cyclostationary behaviour of the signals was proposed. The research was also used to detect cyclostationary signals leading towards development of cyclostationary detectors.

To implement the cyclostationary detector, cyclostationarity features of the signals are used [37]. If a signal is found in the channel, cyclic correlation values have peaks in it. If there are no peak(s), it implies that spectrum band is idle and no signal is present at the observation

time. Test statistics are usually formed using the values in spectral density of correlation. For better calculations of correlation spectral peaks values large number of samples are important. A better signal detection is carried out in this way. Cyclostationary processing has added benefit of insensitivity to lower SNR and without demodulating the received signal it can detect it [38]. As the implementation is considered, cyclostationary detector is fast fourier transform (FFT) based and degrading SNR issues are avoidable as variance of noise is not needed in cyclic spectral analysis. This gives added advantage over the conventional energy detection method. The trade-off between good performance and high efficiency is always there for the implementation of the detection system. It is emphasized in the research literature to use longer length of observation data in order to have better signal detection estimation. Cyclostationary processing is beneficial in two important aspects. The one is its less sensitivity to low SNR (Signal to Noise ratio) and the other one is that it does not require any demodulation of the signal under consideration for extracting significant features for signal detection. Different techniques for signal detection developed in the literature have exploited the inherent properties of the parameters resulting in cyclostationary analysis. Symmetric nature and cyclic frequency location spectral peaks are two examples. These properties appear in the spectral density of the cyclostationary signal. Other techniques using complex processing for pattern matching based feature verification were also developed. The main disadvantages are high resolution analysis and complex computational requirements making them void for usage in faster spectrum sensing modules of cognitive radio designs. One such design is a satellite cognitive radio. Till date, energy based detection and processing on PSD (Power Spectral Density) of the received spectrum has been utilized for the subject of spectrum sensing for satellite cognitive radios. [42]-[43].

2.2 Specific Signal Detection Techniques

Cyclostationary signals when analysed produce features as a result. Optimum detection has been done by comparing the ideal spectral density signatures for OFDM scheme QPSK carriers with the received one in [2]. This comparison scheme has good performance in terms of detection probability under low SNR. Also, only one FFT calculation block both for OFDM carrier generation and spectral density calculations was used reducing hardware resource utilization. But it requires high resolution complex computations in order to detect the features similar to the ideal signatures of OFDM features. Timing mismatches causing feature attenuation were avoided in [5] by extracting feature vectors for each modulation type considered in the analysis. These feature vectors were compared separately with the

calculated feature vector for the input signal for detecting the signal. The technique was proved to be robust for mitigating timing mismatches effects on the features in the spectral density. The pre-processing stage introduced to estimate the symbol rate of the incoming data had Haar wavelets. Wavelets were used to provide blindly estimated symbol rate by measuring the phase transitions from symbol changes. The frequency seperation between transitions provides the estimated symbol rate Interpolated new symbol rate is used to calculate the cyclic spectrum. The proposed technique assumed a prior known carrier frequency. Wavelet based symbol rate estimation, spectral density at specific locations and comparison of feature vectors for different modulations made the technique very complex. In [6] SDR (software defined radio) based cyclostationary analysis had been done. Coherence function was used to normalize the spectral density and carrier frequency was estimated. Spectrogram of the modulated data is used to detect the presence of the signal graphically. Carrier frequency and bit rate of the input signal was successfully estimated. The presented work enlightens only the various parameters that can be estimated using the spectral density using real time data captured from USRP. The experimentation setup of this paper provides the basic setup requirements and procedures for capturing real time data in this research. Parallel implementation of cyclostationary mathematical model had been carried out in [12]. The method adopted was to calculate the spectral density using parallel hardware blocks instead of sequential approach. FAM (FFT Accumulation Method) is used to calculate it. A symmetry test for features in the cyclic spectrum was done to detect the signal. A very low computational time was achieved in estimating the cyclic spectrum using parralel hardware estimators. The parallelism of technique supersedes the serial implementation but the parallel threads required high resolution analysis for symmetric detection. High resolution analysis means incorporating every possible value of cyclic frequency in the analysis. Efficient spectral density algorithm on FPGA was implemented in [17] to perform the cyclostationary analysis of the signals. The detection technique under training mode saves the location of the peaks particularly produced in spectral density in look up tables with memory requirements. High complexity involves when the whole values of the analysed data got compared with the data of the look up tables. FAM algorithm has been successfully implemented on FPGA but for the detection of signal higher memory requirement based look up tables were used. High resolution cyclostationary analysis done to make decision of a signal presence presented in [20] exploited symmetry in the correlation statistics. A blind but complex in computation technique was presented in [23]. It is calculating SCSD (Sum of the magnitude square of the Cyclic Spectral Density). Symmetric property of the cyclic spectral density, magnitude

square, convolution between frequency shifted signal and differentiation was done to reach at the peaks and jumps in the cyclic frequency on the basis of which detection decision is done. Additional computational complexity added with two fast fourier transforms (FFTs) and inverse fourier transform (IFT). Blind hierarchical SDR based detection using ratio of high resolution coherence function and higher order cumulants was proposed in [27]. Practical classifier values for the cumulants were presented for BPSK, QPSK and 16-QAM modulations. The spectral density was calculated using spectral coherence function. Energy detection was used to determine the signal in the channel at the desired frequency. Then using detailed coherence function ratios for BPSK, QPSK and 16-QAM modulations were calculated. Threshold for detection was set using the mean point of the probability density function of the three modulations. The application of cumulants on the I and Q samples proved to be a good modulation classifier. Similar application of cumulants has been shown in the presented research using the resultant feature vector from the proposed technique as the input to the cumulant algorithm. Third order cyclic cumulants for one value of cyclic frequency (the frequency of periodic repetitions) were presented in [29]. Cyclic cumulants on BPSK modulation were applied in [30] to analyse the features of BPSK modulation using higher order statistics. Covariance based matrix was calculated to detect the signal numerically by comparing with a predetermined threshold. As the order of the calculation statistics increases along with covariance matrix calculations, less efficient the technique becomes in terms of computational requirements. Circular correlation stage addition was proposed in [33] before the FFT stage in cyclostationary detector resulting in enhanced features achieved under lower SNR at the expense of higher computational complexity. The circular correlation stage provides a zero valued result when noise is input to the system due to random nature of the noise signal. When a true signal with cyclic periodicities inserted then it shows real values for cyclic correlation. In this way the spectral density contains features in it which were searched by the detector in terms of numerical values. Resulting enhanced features in spectral density were presented for different modulations. Single cyclic frequency based high resolution analysis presented in [35] utilizes the maximum value of spectral density at an assumed single cycle frequency as the function of the carrier frequency with assumption of known carrier frequency and modulation type for the analysed signal. Whole spectral density calculations were avoided and significant feature was achieved at low SNR. Detection decision is done using the threshold value achieved in case of noise and in case of signal plus noise values. The technique works with the assumption of AWGN noise. Wavelets processed spectral feature detection in the graphical plot of spectral density was

carried out in [39]. Reconstruction of spectral density plot was done by utilizing the smaller number of samples using non-linear or convex reconstruction algorithms. This is known as compressed sensing technique. The noise produced by the reconstruction process was removed by treating the resulting spectral density as grey image plot using Wavelets. Noise reduction and good application of Wavelets in RF domain was achieved but higher complexity with the use of two dimensional Haar wavelets was unavoidable. Spectral density estimations were carried out by using the compressed orthogonal reconstruction from samples. ANN (Artificial neural network) trained in [40] were used to detect and classify modulation type of the inputted cyclostationary signals. Three layered ANN structure was used. Coherence function was first applied to get the training data for ANN. The proposed technique proved to be working well with good probability of detection and classification of the signal. Coherence function and ANN implementation makes the technique computationally demanding. In [44], cyclostationary analysis for under water acoustic communication has been presented. The modulation format of BPSK and QPSK were analysed. The detection technique works by estimating the spectral density of the input signal using dynamic multi resolution spectral correlation function. In this technique SCF is estimated with low resolution for cyclic frequency in all the regions and with high resolution at specific locations for cyclic frequency where significant features appear. Peak ratios for BPSK and QPSK are calculated by dividing the peak magnitude at cyclic frequency and frequency axes. Modulation detection was achieved in under water acoustic communication using this cyclostationary analysis detection technique. Higher detection probabilities were resulted by experimenting on real data. The technique has been found susceptible to doppler and noise effects of underwater scenario and in practice it is more dependent on the ratio statistical values. Also, large samples were used to perform the detection of modulation.

It is evident from the above discussion on different novel techniques that cylostationary analysis is computationally complex and has statistical dependence such as variance and mean due to guassian nature of communication signal and noise. There is still room for new methods based on SCF of the modulated signals for detection. In connection to cognitive radios for satellite very less emphasis is found in the literature. So, this research fills the gap and focused on a less complex cyclo-detector using low resolution and less number of samples spectrum sensing scheme. The proposed new scheme must be well performing but must use fewer resources in terms of computational operations. Also, HOS cumulants have never been tested on the features of the spectral density. The hypothesis can be formulated

with the fact that if a signal sample can be used to classify modulation type applying HOS cumulants then considering the feature numerical values in form of an input vector should result in some form of static ranges or values which can help in classification of the modulation type for the detected signal.

In the coming chapter, the basis of the methods and mathematical description of cyclsotationary analysis along with an efficient time smoothing algorithm for estimating the SCF with low resolution has been presented.

Chapter 3. **Cyclostationary Analysis and FAM algorithm**

In this chapter mathematical model of the cyclostationary analysis has been presented. First detailed discussion on the involvement of second order statistics in determining the cyclostationary features was done. A derivation of spectral correlation density is presented. In the end, an efficient previously proposed time smoothing algorithm known as FFT accumulation method (FAM) with operational details is discussed.

3.1 Background

In satellite communication, modulated signals are used for different applications utilizing the band of frequencies supported by the satellite. These modulated signals are cyclostationary in nature [1]. Cyclostationary features are caused by the periodicity in the signal due to multiplexing, product modulation, coding and preambles induced in the generation process [1]. Signal's mean and autocorrelation shows periodic features. Cyclostationary based algorithms can be used to detect signals in a band exploiting cyclic correlation function and can differentiate between noise and signals [7] cyclic autocorrelation function (CAF) is calculated for a cyclostationary signal which is a Fourier series coefficient $R_x(\tau)$. CAF exhibits the correlation between widely separated components because of the spectral redundancy due to periodicity [12]. Second order statistics of the signal are calculated using the Fourier coefficients in terms of its CAF and SCF.

3.2 Cyclic Autocorrelation Function

The periodic autocorrelation function can be expressed as:

$$R_x(t,\tau) = E[(x(t)x^*(t-\tau))] \qquad \text{Equation 3-1}$$

For a cyclostationary signal $R_x(t,\tau)$ is periodic and its Fourier series decomposition yields:

$$R_x(t,\tau) = \sum_\alpha R_x^\alpha(\tau)e^{i2\pi\alpha t} \qquad \text{Equation 3-2}$$

Where α is the cyclic frequency. The cyclic frequency α is the occurrences of the correlation due to periodicity in time domain [1]. Fourier coefficient $R_x^\alpha(\tau)$ is called the CAF and can be expressed as:

$$R_x^\alpha(\tau) = \lim_{T\to\infty} \frac{1}{T}\int_{\frac{-T}{2}}^{\frac{T}{2}} R_x(t,\tau)e^{-i2\pi\alpha t}dt \qquad \text{Equation 3-3}$$

Where, T is the observation interval for the signal.

$R_x(t,\tau)$ can be replaced by symmetric delay conjugate product and can be expressed as:

$$R_x^{\alpha}(\tau) = \lim_{T\to\infty} \frac{1}{T} \int_{\frac{-T}{2}}^{\frac{T}{2}} X\left(t+\frac{\tau}{2}\right) X(t-\frac{\tau}{2})^* e^{-i2\pi\alpha t} dt \qquad \text{Equation 3-4}$$

Cyclic correlation in time domain is between two frequencies shifted x (t) values which in frequency domain are separated by α.

Let $u(t) = x(t)e^{-i\pi\alpha t}$ and $v(t) = x(t)e^{i\pi\alpha t}$ are two shifted version of $x(t)$.

$$R_x^{\alpha}(\tau) = \lim_{T\to\infty} \frac{1}{T} \int_{\frac{-T}{2}}^{\frac{T}{2}} u\left(t+\frac{\tau}{2}\right) v(t-\frac{\tau}{2})^* \, dt \qquad \text{Equation 3-5}$$

The fourier transform of the CAF of x(t) is defined as the spectral correlation density (SCF). SCF is the cyclic spectrum at a given cycle frequency α. It is the density of the correlation between two spectral components separated by an amount equal to cycle frequency. SCF is also referred to as cyclic spectral density (CSD). The CSD function produces peaks when cycle frequency is exact multiple of fundamental frequency due to correlation [7].

3.3 Spectral Correlation Function

The SCF from the CAF is given as:

$$S_x^{\alpha}(f) = \int_{-\infty}^{\infty} R_x^{\alpha}(\tau)\, e^{-i2\pi f\tau} \, d\tau \qquad \text{Equation 3-6}$$

In terms of symmetric delay conjugate product between frequencies $(f+\frac{\alpha}{2})$ and $(f-\frac{\alpha}{2})$ for T interval, SCF in Eq. 3-6 becomes:

$$S_x^{\alpha}(f) = \lim_{\Delta t\to\infty} \lim_{T\to\infty} \frac{1}{\Delta t}\frac{1}{T} \int_{-\frac{\Delta t}{2}}^{\frac{\Delta t}{2}} X_T\left(t, f+\frac{\alpha}{2}\right) X_T^*\left(t, f-\frac{\alpha}{2}\right) dt \qquad \text{Equation 3-7}$$

Where, $X_T(t,f)$ is the spectral component of x(t) given as :

$$X_T(t,f) = \int_{t-\frac{T}{2}}^{t+\frac{T}{2}} x(t) e^{-i2\pi f}\, dt \qquad \text{Equation 3-8}$$

The calculated SCF is viewed on a bi-frequency plane as a function of frequency f and cyclic frequency α . A range for spectral frequency f is from $-\frac{f_s}{2}$ to $\frac{f_s}{2}$ and α is from $-f_s$ to f_s .

Modulated signals have unique features pattern in their SCF that can be utilized for signal detection [8].

3.4 FFT Accumulation Method

FFT accumulation method (FAM) is an algorithm for SCF calculation based on time smoothing method. Time smoothing method is an efficient method for SCF calculation than frequency smoothing method [9]-[11]. FAM method calculates the fourier transform (FT) of the time smoothed correlation product of the spectral components.

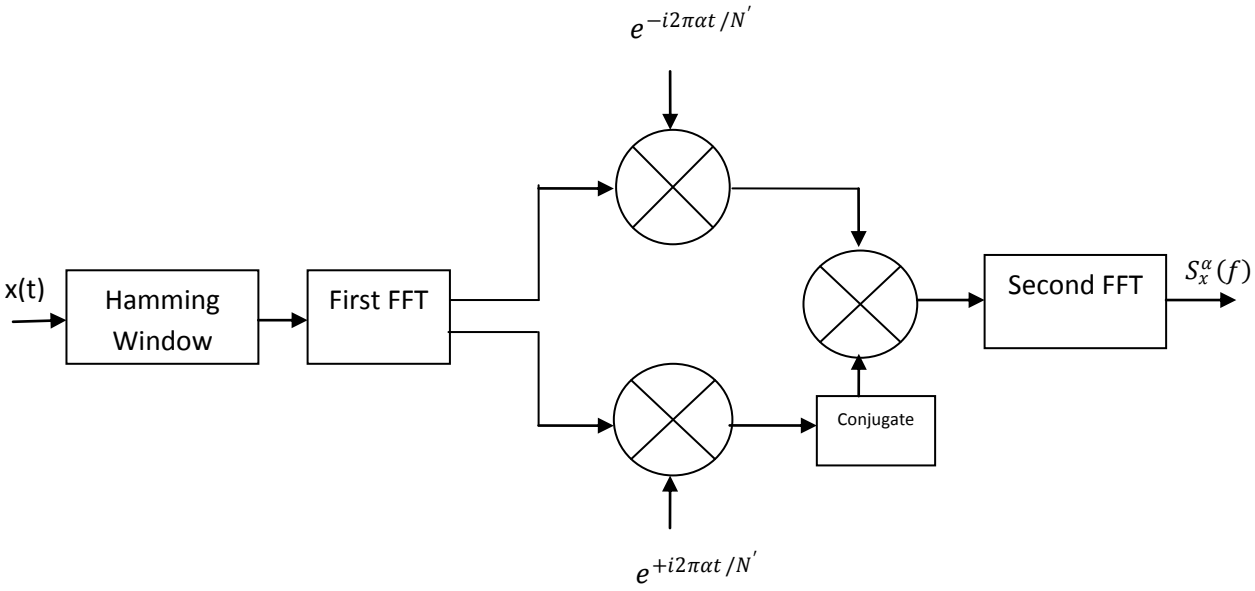

Figure 3-1: Time Smoothing FAM Procedure

Input signal x(n) in Fig. 3-1 is divided into blocks by Hamming window for reducing the spectral leakage. Complex demodulates are estimated efficiently by FFT covering all the samples in the input. Frequency shift is done to convert the signal into baseband. A step size is used instead of continuous slid through samples. Product sequences from the calculated components and complex conjugate are formed followed by a second FFT for time smoothing [21]. The first FFT size is determined by the frequency resolution Δf and second FFT size is determined by cyclic frequency resolution Δα.

$$N' = \frac{f_s}{\Delta f} \qquad \text{Equation 3-9}$$

$$P = \frac{f_s}{L\Delta\alpha} \qquad \text{Equation 3-10}$$

Where, N' and P are the first and second FFT sizes respectively. f_s is the sampling frequency.

Next, using the presented cyclostationary theory, ideal SCF of BPSK, QPSK and 16-QAM modulation are presented. The theoretical values of the feature peaks as they may appear in the spectral density and the parameters on which the values of the peaks depend are identified. Locations for typical feature points in the cyclic frequency are identified. The reasons behind the number of peaks as they may appear in the practical scenarios are highlighted for higher order QPSK and 16-QAM modulation formats.

Chapter 4. **SCF of BPSK, QPSK & 16-QAM Modulations**

Ideal features of the SCF for the subject modulation types are presented in this chapter. Using the cyclostationary concepts and definitions, features in the SCF of BPSK, QPSK and 16-QAM modulations can be mathematically estimated as follows.

4.1 BPSK Modulation

For BPSK modulated signal $y(t) = a(t)cos(2\pi f_c t + \phi_0)$, SCF according to [23] & [36] can be expressed as:

$$S_y^{\alpha}(f) = \begin{cases} \frac{1}{4}[S_{\alpha}^{0}(f - f_c) + S_{\alpha}^{0}(f + f_c)], & \alpha = 0; \\ \frac{1}{4}e^{j2\phi_0}S_{\alpha}^{0}(f), & \alpha = 2f_c \\ \frac{1}{4}e^{-j2\phi_0}S_{\alpha}^{0}(f), & \alpha = -2f_c \end{cases} \qquad \text{Equation 4-1}$$

Where α is the cyclic frequency, ϕ_0 is the shift in phase and S_{α}^{0} is the Fourier transform of the autocorrelation $R_{\alpha}^{0}(\tau)$.

It is clear from the above estimate that the BPSK will show total four peaks. Two in the cyclic domain where $f = 0$ and two in the frequency domain where α = 0 in the bi-frequency plot of SCF.

4.2 QPSK Modulation

For QPSK modulated signal $y(t) = \frac{1}{\sqrt{2}}[a(t)\,cos(2\pi f_c t + \phi_0) + b(t)cos(2\pi f_c t + \phi_0 + \frac{\pi}{2})]$. The inphase $a(t)$ and quadrature $b(t)$ can be viewed as two separate BPSKs respectively. So SCF for QPSK can be given as:

$$S_y^{\alpha}(f) = \left\{\frac{1}{4}[S_{\alpha}^{0}(f - f_c) + S_{\alpha}^{0}(f + f_c)], \quad \alpha = 0; \right. \qquad \text{Equation 4-2}$$

QPSK will be having two peaks in frequency domain where α = 0. This is due to the cancelation of in-phase part and quadrature part in cyclic frequency domain.

4.3 16-QAM Modulation

For 16-QAM modulated signal $y(t) = c(t)\,cos(2\pi f_0 t) - d(t)\,sin(2\pi f_0 t)$. 16-QAM will have two peaks in the frequency domain at α = 0. Moreover, if the in-phase and quadrature part cancels out each other completely, then there will be no peaks in the cyclic frequency domain. For the case of no or little subtraction between in-phase and quadrature components, peaks may appear at locations in frequency domain.

A graphical representation of the ideal SCF of the BPSK plotted against f and α can be seen in Fig. 4-1. The circles in blue colour depicts the peaks in the SCF at specified values of cyclic frequency α, frequency resolution f and the carrier frequency f_c.

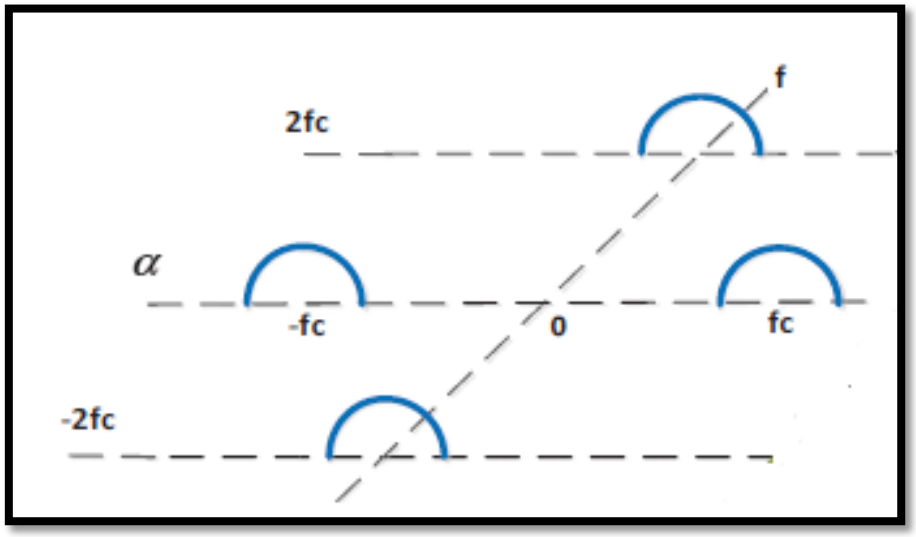

Figure 4-1: A graphical representation of Ideal BPSK SCF

BPSK modulation shows four peaks according to Eq. 4-1. If proper values for the cyclic frequency resolution and frequency resolution are set in the analysis, ideal SCF is obtained for modulated signals present in the sampled data input to the analysis algorithm. Cyclostationary features then can be used to detect the signal from the noise.

With such detailed analysis and idea of direction of research in cyclostationary analysis of the signals now a simple, low resolution spectrum sensing technique with application of cumulants on the resulting spectral density feature vector for classification of the modulation of the detected signal is presented in the following chapter.

Chapter 5. **Proposed Detection Technique**

Spectral correlation function $S_x(f,\alpha)$ is a two-dimensional function of frequency and cyclic frequency when calculated practically. It shows particular spectral peaks at certain frequency and cyclic frequency locations due to cyclostationarity. These peaks are particular features represented by SCF for particular modulated signals as in our case it is BPSK, QPSK & 16-QAM. The main idea behind devising a new technique is to enable a logical decision block and quantify the features shown by the SCF. For this purpose different techniques for detection have been proposed in [2, 12, 13, 16, 18 & 20]. All of these techniques in the literature use the calculated SCF further process it and reach at the detection hypothesis solution. One more method is to calculate high resolution SCF [2] & [12] and use its inherent properties at particular cyclic frequency locations to detect presence of signal. In the proposed method first SCF is calculated using FAM algorithm. The frequency and cyclic frequency resolutions used are very low i.e. in order of KHz which is far greater in value from different recent and former approaches using frequency resolutions in hertz (Hz). Secondly, only 1024 maximum and 600 minimum samples have been used as input to the FAM algorithm. In simulation chapter details of the parameters of FAM algorithm has been presented. SCF containing features in its two dimensional bi-frequency plane plot for discrete input data can be expressed as cyclic periodogram [14],

$$S_x(f,\alpha) = \frac{1}{N}\sum_{n=0}^{N-1} X_t(t_n,f)X_T^*(t_n,f+\alpha) \qquad \text{Equation 5-1}$$

Let's define M as the maximum value in the calculated SCF so,

$$M = \max_{2-\text{d index}} S_x(f,\alpha) \qquad \text{Equation 5-2}$$

Now, we define a normalized SCF as:

$$S_x(a,b) = S_x(f,\alpha) * \frac{1}{M} \qquad \text{Equation 5-3}$$

The features in the SCF can be extracted into a calculated column vector as:

$$V_i(K) =$$

$$[Maximum\ Value\ of\ every\ column\ Index\ (1,2,3,\ldots.a)] \xleftarrow{\max_{(Row\ \ Wise\ \ shift\ \&\ compare\ )} S_x(a,b)}$$

Equation 5-4

Where 'K' have values ranging from 1 to a. 'a' represents the number of rows in SCF.

The proposed detection uses only half of the values in the calculated vector to detect the presence of signal or noise in the analysed data. This reduces the calculation complexity from 'N' vector point analysis to 'N/2' as in [18].

The calculated vector $V_i(K)$ above is used by the detection block to generate the result of the hypothesis of signal and the noise in the captured spectrum band. The significant features of the SCF are presented in form of values in the index of vector V_i . This vector is a column vector. The values in the vector are in the range from $0 \underset{\text{to}}{\rightarrow} 1$. Spectral peaks in the SCF at the locations of $(f=0,\ \alpha=\pm 2f_c)$, $(f=\pm f_c,\ \alpha=0)$, $(\alpha=0)$, $(f=\pm f_c, \pm 0.5f_c, \alpha = \pm 2f_c, \pm f_c)$ which are generally seen in the modulated data as in [1, 5, 12, 16 & 21] are gathered in the calculated vector. Points of spectral correlation have values near to one. In case of noise, the SCF shows features only at α=0 for whole values of f [23]. The calculated vector therefore, has more values near one. The distinction between a signal and noise thus can be made by using this response of the vector $V_i(K)$. A threshold value γ is defined which is used to identify the number of values qualifying for distinguishing between noise and signal response. By experimentation, the values of interest in the vector are those passing $\gamma > 0.5$ threshold.

Let the hypothesis for detection be

$$H_0 = n(t) \qquad \text{Equation 5-5}$$

$$H_1 = y(t) + n(t) \qquad \text{Equation 5-6}$$

Where n(t) is the noise and $y(t) + n(t)$ is signal with noise.

The decision is done for the two hypotheses above by calculating:

$$H_0 = No.of\ Values\ > \gamma = \frac{N}{2} \qquad \text{Equation 5-7}$$

$$H_1 = No.of\ Values\ > \gamma \neq \frac{N}{2} \qquad \text{Equation 5-8}$$

The detection procedure works as follows:

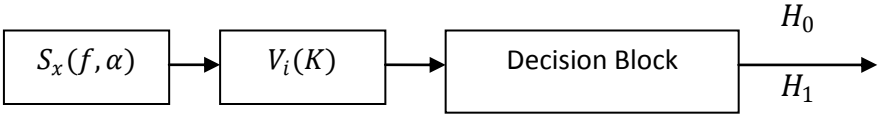

Figure 5-1: Block Diagram of the detector

After calculating the SCF as shown in Fig. 5-1, the vector $V_i(K)$ is extracted out containing the normalized SCF features in form of magnitudes ranging between 0 and 1. The decision block then counts the number of values in the vector above $\gamma > 0.5$ threshold level to decide between H_0 or H_1.

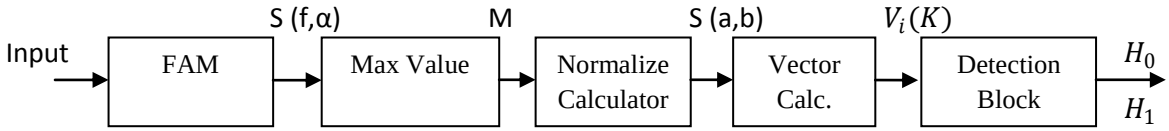

Figure 5-2: Block Diagram of the technique

The working of the algorithm can be summarized in the following steps.

1. Estimate the SCF of the input signal using the low resolution values for frequency and cyclic frequency as parameter inputs to FAM. The resolution values are listed in Table 3 in chapter 7.
2. Extract the maximum feature value's magnitude in the two dimensional plot of the calculated SCF using sort and compare in a nested conditional loop.
3. Normalize the whole SCF values by using this maximum value obtained in step 2.
4. Now take a one dimensional vector and extract the maximum value in magnitude from the SCF which is a matrix containing rows and columns. Sort and compare values by scanning the columns in rows.
5. Put only maximum value of the row in the vector. The vector would contain only values in the magnitude range from 0 to 1.
6. Now a search for the values passing the defined threshold is done.
7. Using the defined hypothesis for H_0 and H_1. If the number of peaks passing the threshold exceeds half of the number of values in the vector then detection of noise is declared else presence of the signal is declared.

5.1 Alternate to Spectral Coherence Function (SOF)

The coherence function is especially useful for cyclic frequency detection, since the coherence value is independent of the absolute power levels of the signals from the data signal $y(t)$, which simplifies choosing the threshold for detection [16] & [21]. Additional advantage of SOF (being the normalized version of SCF) is that it helps in removing the channel effect [16]. In literature a normalized version of the SCF is obtained for detection of signals using the Spectral Coherence Function (SOF) is given as:

$$C_y^{\alpha}(f) = \frac{S_y^{\alpha}(f)}{\sqrt{S_y^{0}\left(f+\frac{\alpha}{2}\right)S_y^{0}\left(f-\frac{\alpha}{2}\right)}} \qquad \text{Equation 5-9}$$

If we take a closer look at the Eq. 5-9, it shows clearly that first SCF has to be estimated and at different cyclic frequency shifts the product value of α = 0 SCF is used to calculate the coherence function $C_y^{\alpha}(f)$. Summarily, it is ratio of the whole bi-frequency SCF to the square root of the product of cyclic frequency shifted values at α = 0. These values can also be referred to as power spectral density (PSD) values [1]. This normalization method in comparison to the proposed technique implicates high computational complexity even if we select certain cyclic frequency locations such as α = $2f_c$ for calculating the denominator products. In the proposed technique of this research, simply maximum value of SCF in the bi-frequency plane is calculated and whole SCF of the bi-frequency plane is divided by this value using Eq. 5-3. However, in this research the proposed method for detection has all the advantages offered by SOF with lesser amount of computational resources unlike the coherence function.

5.2 Fourth-Order Cumulants on Calculated Feature Vector for Modulation Classification

The spectrum sensing approach so far proposed has the ability to successively detect signal in the band of interest. But the type of modulation of the detected signal is unknown. One of most extensive methods used in the literature for modulation recognition is by using HOS (Higher order statistics). This is done by calculating the cyclic cumulants of 4th and above orders of the signal captured for detection purpose [24]-[28]. The type of modulated signals in the presented work includes BPSK, QPSK and 16-QAM modulations. For BPSK only second-order statistics are enough to classify it. But for the case of QPSK and 16-QAM modulations, it lies in the higher order statistics i.e. 4th order cumulants are required to classify between these types of higher modulations [27].

In literature the modulation classification is done by first using the captured data (which can be complex valued or real valued data) to detect signal via energy detection method [24] & [26]. Then cumulant values for third [29] or 4th order cumulants are estimated for different modulation schemes [27]. The Cumulant values thus estimated are used to classify the modulation types. It is evident from this approach that cumulants provides characteristic values different for different modulation types which helps in modulation recognition [28].

For a random complex process z(n), second order moments are given as:

$$C_{20} = E|z^2(n)| \quad \text{Equation 5-10}$$

$$C_{21} = E[|z(n)|^2] \quad \text{Equation 5-11}$$

E[.] here is showing expected value of the z(n) random process .

Fourth order moments and cumulants can be written in the following three ways [24]. 4th order cumulants can be defined as:

$$C_{40} = cum\,(z(n), z(n), z(n), z(n)) \quad \text{Equation 5-12}$$

$$C_{41} = cum\,(z(n), z(n), z(n), z^*(n)) \quad \text{Equation 5-13}$$

$$C_{42} = cum\,(z(n), z(n), z^*(n), z^*(n)) \quad \text{Equation 5-14}$$

For random variables a, b, c, d the fourth order cumulants can be written as:

$$cum(a, b, c, d) = E(abcd) - E(ab)E(cd) - E(ac)E(bd) - E(ad)E(bc) \quad \text{Equation 5-15}$$

Eq. 5-12, 13, 14 can be used to express $C_{40}, C_{41} or\, C_{42}$ using second and fourth order moments of z(n) [24] [27].

The estimates of cumulants in Eq. 5-14 using estimates of corresponding moments are given as:

$$\widehat{C_{21}} = \frac{1}{N}\sum_{N=1}^{N} |y(n)|^2 \quad \text{Equation 5-16}$$

$$\widehat{C_{20}} = \frac{1}{N}\sum_{N=1}^{N} y^2(n) \quad \text{Equation 5-17}$$

$$\widehat{C_{40}} = \frac{1}{N}\sum_{N=1}^{N} y^4(n) - 3\widehat{C_{20}^2} \quad \text{Equation 5-18}$$

$$\widehat{C_{41}} = \frac{1}{N}\sum_{N=1}^{N} y^3(n)y^*(n) - 3\widehat{C_{20}}\,\widehat{C_{21}} \quad \text{Equation 5-19}$$

$$\widehat{C_{42}} = \frac{1}{N}\sum_{N=1}^{N} |y(n)|^4 - \widehat{C_{20}^2} - 2\widehat{C_{21}^2} \quad \text{Equation 5-20}$$

Where the subscript ^ denotes sample average.

Alternatively, in terms of moments above estimates can be written as in [28]:

$$M_{pq} = E[X(t)^{p-q}X^*(t)^q] \quad \text{Equation 5-21}$$

(*) means the complex conjugate. Cumulants C_{40}, C_{41} & C_{42} then can be expressed as:

$$C_{40} = M_{40} - 3M_{20}^2 \quad \text{Equation 5-22}$$

$$C_{41} = M_{41} - 3M_{20}M_{21} \quad \text{Equation 5-23}$$

$$C_{42} = M_{42} - M_{20}M_{22} - 2M_{22} \quad \text{Equation 5-24}$$

So far detailed estimates of cumulants have been presented with special focus on fourth-order cumulants. This is because of the fact that higher order modulations of QPSK and 16-QAM shows feature values on fourth order cumulants. These feature values are used to classify these modulations after a signal is detected. One of the other main reasons for using the fourth order cumulant and not the third order cumulant is that for a random process that is symmetrically distributed, it's third order cumulants are equal to zero. Moreover, higher signal modulations have extremely small third-order cumulant value and larger fourth-order cumulant value so preference is given to fourth-order cumulant [26]. There are theoretical values for the estimated cumulants for different modulations [24] & [25] which can be used to classify the modulations. Practically cumulants were applied in [27] and range for cumulants estimates has been provided by the author. This approach is utilized further in the classification process used in this research.

The application of cumulants after doing cyclostationary analysis re calculates the second order statistics of the signal. Particular modulation formats producing same features in the calculated moments result in the theoretical values of the cumulants. These values are approximately fixed and are used for classification of modulations after a signal has been detected by the spectrum sensing algorithm. In this research, cumulants are directly applied to the real valued vector calculated from the SCF considering it as a symmetric zero mean random variable which is having approximately a normal distribution. Its cumulant analysis being easy operator is preferred over its moments [25] for characterizing the shape of the distribution [24]. The calculated vector serves as the random process input to the cumulants instead of the captured signal say $y(n)$. In **Error! Reference source not found.** magnitudes of he FFT values obtained by calculating the second order statistics were used to calculate the second, third and fourth moments and then using these values respective cumulants can be calculated using Eq. 5-22, 23, 24. Summarily, the idea of testing the calculated feature vector values by considering them as a random variable inputted to the cumulants will provide the required results which are present as we proceed. This application testing of cumulants on the

vector has many advantages. In comparison to second and fourth order moments of a captured complex signal, the calculated vector has reduced calculation size reducing the complexity of cumulants calculation. Secondly, modulation format produces distinct features if cyclostationary analysis is done correctly. The calculated vector has these features calculated in a unique way. So it increases the probability of distinct values as output of fourth order cumulants for different modulation formats. Thirdly, a unique normalization to value equals to one approach is used in the vector so that cumulant values are least disturbed with the amplitude of the feature values and will produce the consistent values as results, normalization of cumulants has also been presented in [24] for the said purpose. All these particular advantages are being utilized while calculating the fourth order cumulant values for BPSK, QPSK, 16-QAM and Noise feature vectors by the algorithm. This helps in simpler, less computational and low on resources detection and classification of modulation signals.

With such a cumulant based classifier, we can have an idea of the authenticity of the primary signal. Whether the signal present at the analysed frequency is allowed to transmit and also we can use this identification for validation of primary user. Suppression activities of unauthorized carriers can be done by the concerned authorities such as military or the signals and frequency regulatory body.

5.3 Advantages of the Extracted Feature Vector

Some of the fringe advantages of the extracted feature vector are that the correlation spectral peaks at locations of f and α are all present in it. So when compared to noise vector, we have only certain peaky points in the vector. At low resolution, these peaky points are significant only and not there numbers of occurrences at particular locations on which many techniques are dependent as we see in the literature. There are no special pre processing blocks, Wavelets or special high resolution analysis on particular values of cyclic frequency. There is no need for estimating the variance matrices. The said vector is not statistically bound. SCF has been estimated with low resolution FAM. Then, features are extracted from SCF in a vector with normalized values and by comparing and sorting only largest value in a row. Due to normalization, effects of noise variance are diminished as in [14].

The next chapter presents detailed experimentation setup used in this research. Different approaches for capturing signals and verifying the working performance of the proposed technique are discussed in details.

Chapter 6. **Experimentation Setup**

The focus of this work is on cyclostationary analysis of signals that are used in practice by satellite uplink channels. In order to claim the use of the proposed detection technique in CRs for satellite, the experimentation setup should have modern SDR and CR development platforms through which signal generation and acquisition be carried out. MATLAB as being renowned simulation and analysis software platform is then used to validate the devised technique. The details of the setup and special considerations follow in the next sections.

6.1 Experimentation

The main concern of this research is to process the modulated signals used in a real satellite scenario, so the experimentation involves the capture of signals from the valid sources instead of generating them in the simulation software. To gain a deeper insight into the fulfilment of requirements, a flexible CR implementation platform is used [2]. The results are produced by analysing both the AWGN and multi-path fading channels [16]. The first approach selected for the purpose of experimentation is to generate the three modulations using the Agilent technologies E8267D signal generator. It is a renowned fact that using the signal generator at the input of the satellite RF link chain, a simple modulated carrier can be uplinked on the satellite. So keeping this fact in mind, signal generator is configured for generating BPSK, QPSK and 16-QAM modulations and is connected to USRP2 N210 for capturing the modulated data for analysis. A Rohde & Schwarz (26.6-GHz) Spectrum analyser is used to analyse the generated modulation's power spectral density (PSD) and constellation. The generated modulated data is fed into the USRP2, which digitizes the captured data and decimate it. This data is then provided to the computer using the gigabit interface. The SBX daughter card (400-4400 MHz) is used as the RF front-end for the input data to the USRP2. The sampled data is saved in a file sink as in [2] for further processing using Matlab based detection algorithm presented above. The parameters of the generated modulations are listed in the Table 1 and parameters for USRP2 data capture are presented in Table 2 respectively. The GNU radio 3.6 open source software is used to capture the data from USRP2 as it provides a GUI based flow-graph programming model **Error! Reference source not found.**. The se of USRP2 assures the fact that spectrum sensing capability of the proposed research can be utilized in a prospective design of the CR for satellites using modern flexible radio platform.

Parameter	Value
Modulation Type	BPSK, QPSK, 16-QAM
Symbol Rate	2Msps
Data	PN23 (PRBS with $N = 2^{23} - 1$)
Frequency	2.25GHz
Amplitude	-30dBm

Table 1: Modulation parameters on signal generator

Parameter	Value
Sample Rate	10 MHz
Centre Frequency	2.25 GHz
Channel	0, TX/RX
Channel Gain	5dB

Table 2: Parameters for USRP2

For getting the real satellite signals, an RF chain containing parabolic antenna and low noise amplifier + block down converter (LNB) is used. The L band frequency 950-1750MHz output of the reception setup is connected with the spectrum analyser and the USRP2 using a splitter. The real-time satellite spectrum is scanned for carriers of the primary users in 1-4MHz span. This bandwidth is well supported by the USRP2 device **Error! Reference source ot found.**. A broadcasting carrier typically uses a bandwidth of 4MHz. Within this span, the signal of interest is scanned and captured [12]. GNU radio based flow-graph is used to capture the data using USRP2 [5]. The saved samples in the file from the flow-graph are imported in the Matlab for cyclostationary analysis and detection scheme simulation. A block diagram for the experimentation setup is presented in Fig. 6-1 below.

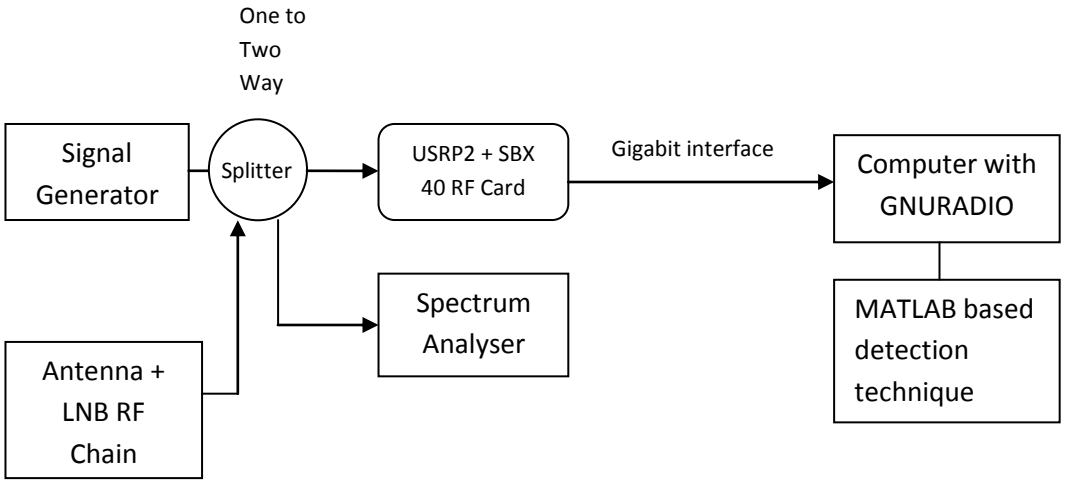

Figure 6-1: Block diagram of the setup where signal generator is used first as input to the splitter (One to two way) for Lab-generated data capturing and analysis and then it is replaced by the RF chain containing 2.4m parabolic antenna and C-band LNB

In Fig. 6-1, the function generator is connected at the input of the USRP2 setup with the spectrum analyser and the PC with GNU Radio flow graph for collecting lab generated modulated data for the analysis. For the real-time satellite signals, the function generator is disconnected and the antenna with C-band 3.4-4.2GHz LNB with LO frequency of 5.15GHz is connected in the input of the USRP2. The centre frequency and the bandwidth for capturing the signal in the band are set by the parameters in the GNU Radio flow graph.

The overall experimentation setup can be summarized in the following main steps:

1. First connect the function generator output with a splitter and configure the function generator with the modulation parameters as listed in Table 1**.**
2. Take the splitter's outputs and connect them to USRP2 and the spectrum analyser respectively. Set the analyser according to the carrier frequency of function generator for taking measurement results.
3. Connect the USRP2 with the computer running GNU Radio flowgraph for capturing the signals in the data file.
4. Now, generate the signals from the function generator, for constellation diagrams and put the spectrum analyser in the vector signal analyser (VSA) mode and set the parameters for the required modulation.
5. Run the flowgraph in the computer for 5 seconds. Measure this time from the first instance of the FFT plot similarly appearing in the flowgraph as it is shown by the spectrum analyser. In the 5 seconds period the recorder file in the GRC flowgraph

will have the minimum number of required samples. Replace function generator with antenna chain and repeat the steps.

6.2 Measurement Results

In Fig. 6-2 (a), setup of the configured and connected signal generator, spectrum analyser and USRP2 are shown. The generated signal from the signal generator is received on the spectrum analyser and USRP2 both using the signal splitter. Fig 6-2 (b) shows the running GNU Radio flow graph which is capturing the signal input to the USRP2 from the signal generator. The FFT plot of the real time generated BPSK modulated signal can be seen in the figure.

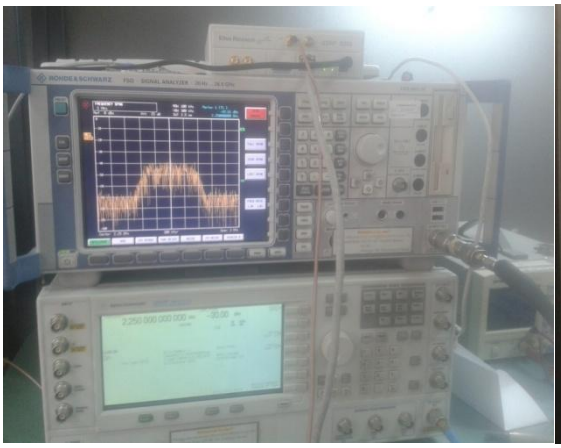

(a)

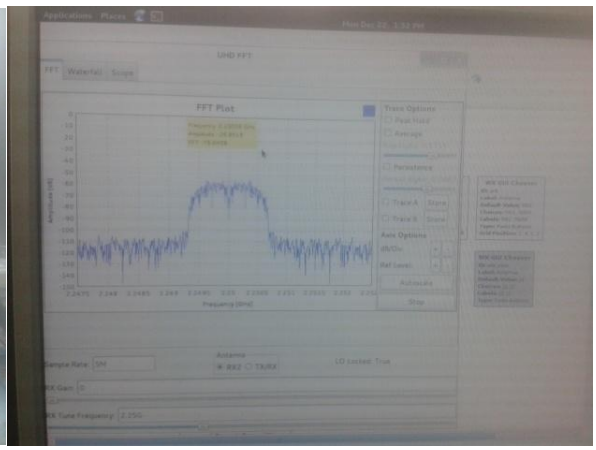

(b)

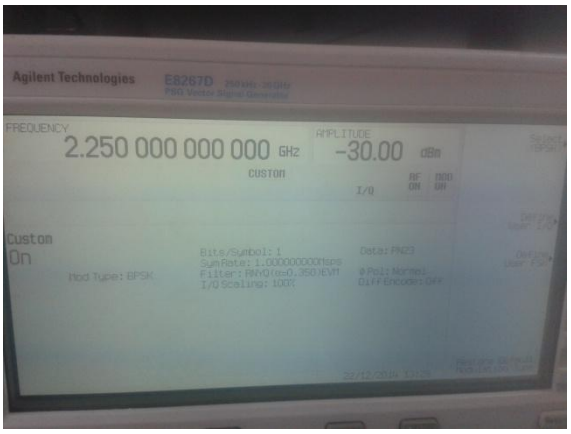

(c)

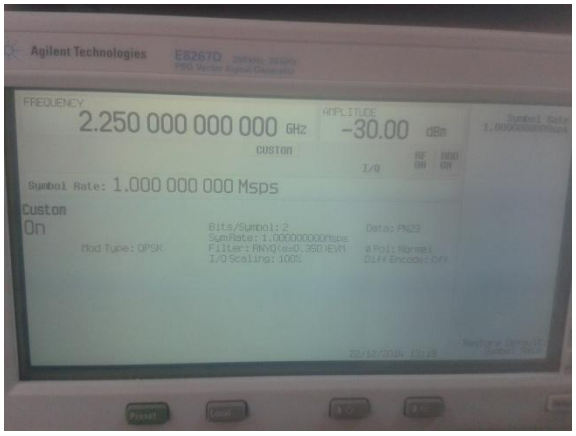

(d)

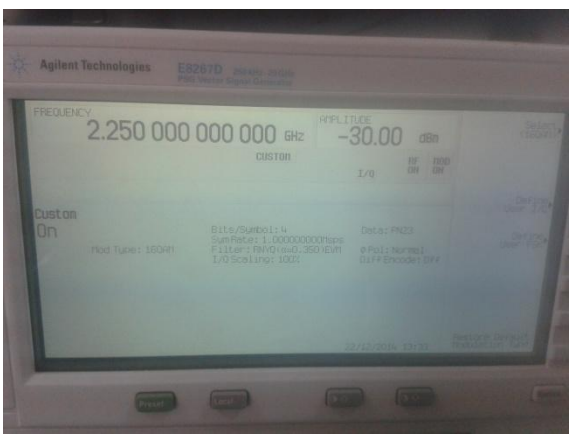

(e) (f)

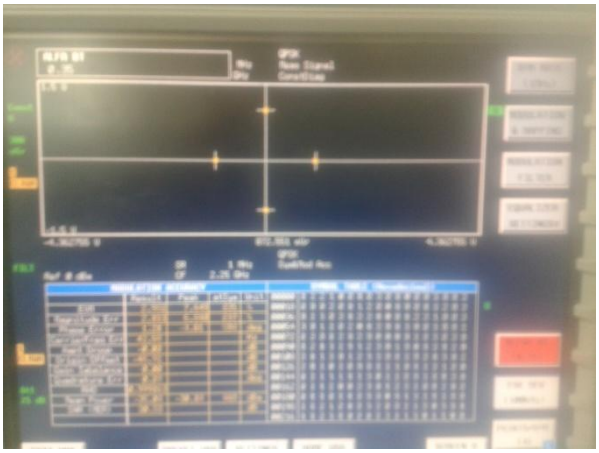

(g) (h)

Figure 6-2: (a) Experimental setup containing USRP2, signal generator and spectrum analyser, (b) FFT plot of signal captured in a file using GRC flowgraph, (c) configuration of signal generator for generating BPSK data, (d) configuration of signal generator for generating QPSK data, (e) configuration of signal generator for generating 16-QAM data, (f) constellation diagram of generated 16-QAM on VSA, (g) constellation diagram of generated BPSK on VSA & (h) constellation diagram of generated QPSK on VSA

Configuration of the signal generator for BPSK, QPSK and 16-QAM modulations is presented in Fig. 6-2 (c), (d) and (e) respectively. The parameters are set according to the listed parameters of Table 1. The modulated data generated is verified on the spectrum analyser in terms of its spectrum and constellation plot. Fig. 6-2 (f), (g) and (h) are showing the constellation plots of 16-QAM, BPSK and QPSK modulated data generated by the signal generator. Same data is input to the USPR2 and collected for testing by the proposed algorithm.

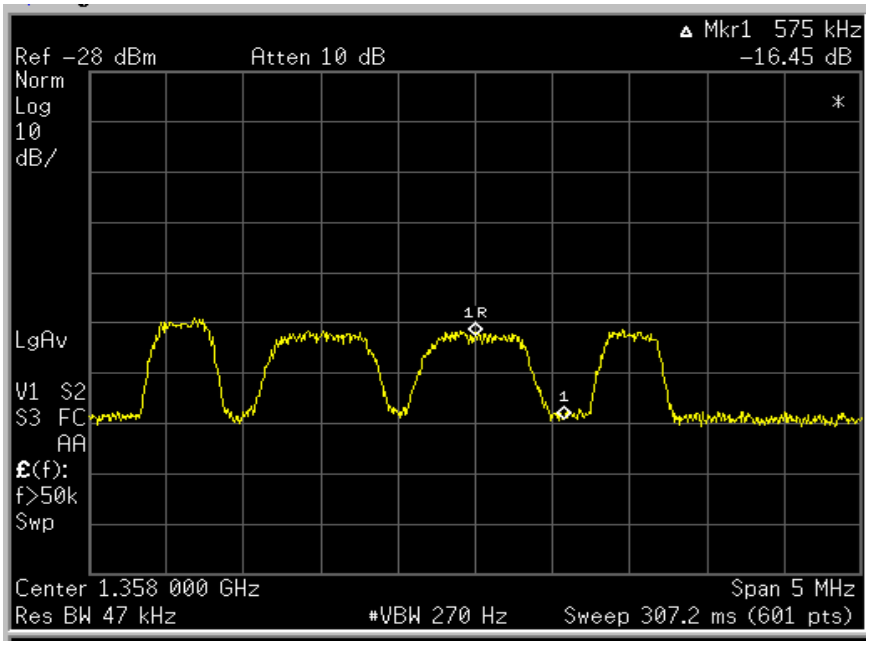

Figure 6-3: Real-time spectrum of satellite on spectrum analyser obtained using the receive only antenna chain with down converted L-band start frequency= 1355.5 GHz, stop frequency = 1360.5 GHz with a 5 MHz span

After experimenting with the lab generated modulated carriers, the discussed receive only chain for capturing the satellite signals was used. The connected spectrum analyser was used to ensure the satellite carriers having the desired modulations of BPSK, QPSK and 16-QAM along with some frequency with no transmission as can be seen in Fig. 6-3 for noise analysis. Zoomed-in views of these carriers are shown in Fig. 6-4. below. The marker labelled as '1' in white colour in Fig. 6-3 is showing the noise floor. Marker labelled as *1R* in white colour is showing the QPSK carrier.

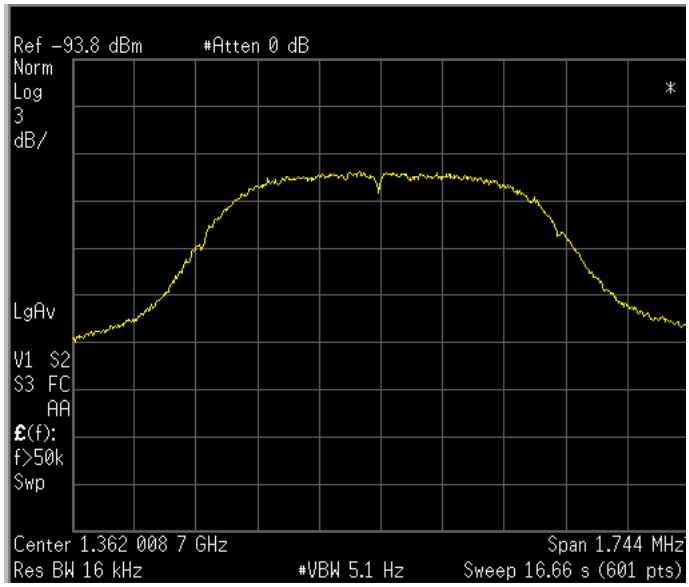
Ref -93.8 dBm
#Atten 0 dB
Norm
Log
3
dB/
LgAv
V1 S2
S3 FC
AA
£(f):
f>50k
Swp
Center 1.362 008 7 GHz
Span 1.744 MHz
Res BW 16 kHz
#VBW 5.1 Hz
Sweep 16.66 s (601 pts)

(a)

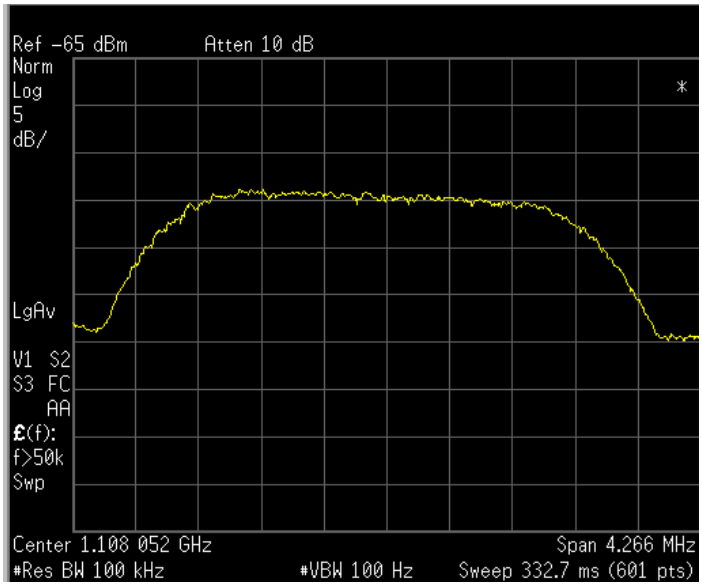
Ref -65 dBm
Atten 10 dB
Norm
Log
5
dB/
LgAv
V1 S2
S3 FC
AA
£(f):
f>50k
Swp
Center 1.108 052 GHz
Span 4.266 MHz
#Res BW 100 kHz
#VBW 100 Hz
Sweep 332.7 ms (601 pts)

(b)

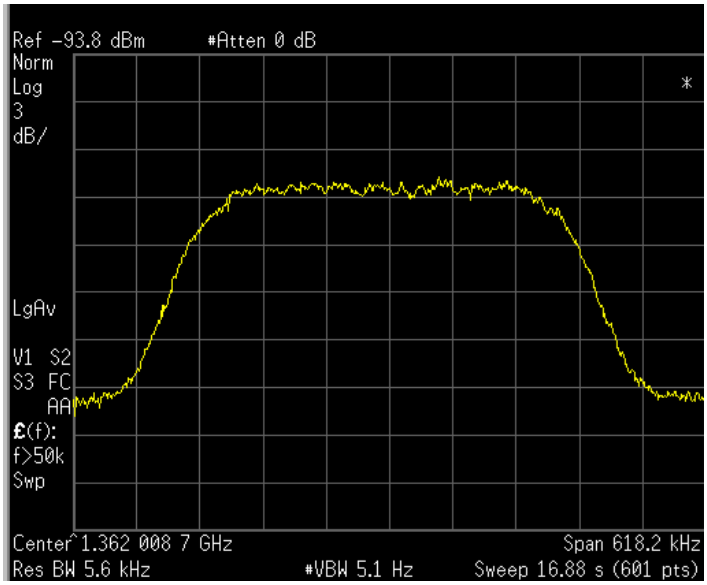

(c)

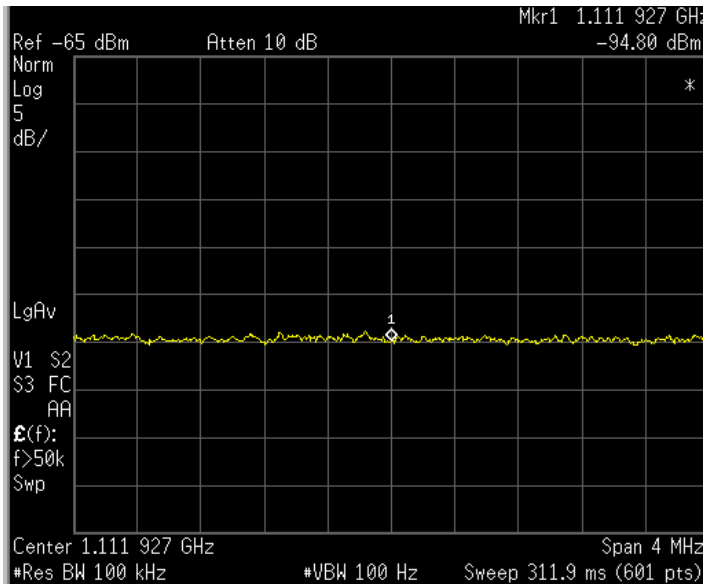

(d)

Figure 6-4: Spectrum of real satellite carriers zoomed-in power spectral density (PSD) view, (a) PSD of BPSK carrier, (b) PSD of QPSK carrier, (c) PSD of 16-QAM carrier and (d) Noise floor of the satellite band

The real-time satellite carriers were captured by connecting the signal generator and USRP2 to the antenna containing the C-band LNB. The spectrum analyser PSD plots for BPSK, QPSK, 16-QAM and noise are shown in Fig. 6-4 (a), (b), (c) and (d) respectively. Particular modulated carrier span is set on the spectrum analyser to get proper view of the power spectral density on the spectrum analyser. Noise is captured by setting the centre frequency of

USRP2 at the location in the satellite band where there is no carrier preset as shown in the spectrum analyser.

The next chapter discusses in detail the obtained results by simulating the algorithm on the captured signals using the USRP2 in GNU Radio and generated by function generator and form real-time satellite signals from the receive only chain. The captured signal files were input to the Matlab implementation of the algorithm.

Chapter 7. **Simulation Results**

The collected samples are analysed and plotted in Matlab [17] using the FAM algorithm and then signal detection is done through the proposed technique. The calculated SCF with low resolution frequency and cyclic frequency is presented for BPSK, QPSK and 16-QAM modulation types. The modulation parameters using the signal generator approach as discussed in the previous chapter on experimentation are set according to the carrier specifications on a real satellite uplink. The SCF for noise and its vector plot is also presented in this chapter. It can be seen from the SCF and calculated vector plots that the proposed technique can effectively identify the difference between a present signal and noise in the sampled data. The proposed technique works effectively even in the multi-path fading channel of the satellite. The parameters for FAM algorithm are presented in Table 3.

Parameter	Value	Unit
Fs	10	MHz
Delta α	20	KHz
Delta f	200	KHz
Np	64	Points
L	16	Points
P	32	Points
N = P*L	512	Points
FFT size	32	Points

Table 3: FAM parameters

The parameters for FAM in Table 3 ensure its low calculation complexity. The platform running Matlab is an Intel Core2duo 2.54GHz processor with 2GB of RAM running Matlab7.0.8.347. The results of SCF for the two approaches along with the calculated vector (obtained using the proposed technique) are being presented in the results chapter.

7.1 Signal Generator Approach

7.1.1 BPSK Modulation

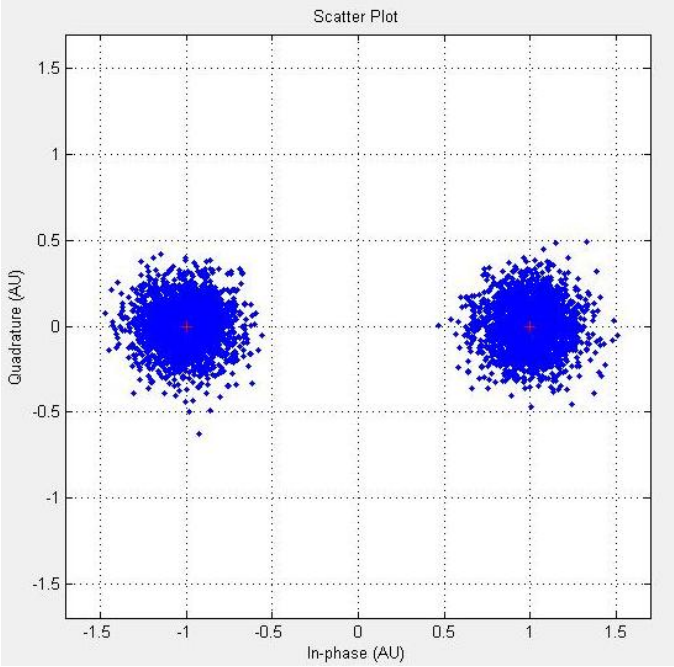

Figure 7-1 Constellation Plot of the BPSK sampled data

Data obtained from the signal generator is first analysed by the constellation plot and proper modulation is assured by getting the scatter plot as shown in Fig. 7-1. The input vector defined in Matlab is used as the input data vector containing sampled data values from the GNU Radio captured file. These files were first recorded during the experimentation and then were used by Matlab to obtain the SCF features and detection results. In Fig. 7-2, the cyclic spectral density of the BPSK signal is shown. The SCF is plotted on z-axis with the bi-plane f and α values on x and y axes respectively. Referring to the mathematical SCF of the BPSK in Chapter 4 Section 4.1, the SCF plot of the BPSK is having four peaks two at $\alpha = 0$ and two at $f = 0$. The frequency f and the cyclic frequency α are normalized to the value of the sampling frequency f_s. If a section through the figure is made where the cyclic frequency $\alpha = 0$, then the spectral power density of the modulated signal is obtained [21]. It is also evident that since α and f values are normalized by f_s and peaks occurs at f_c. That means the peak locations give true f_c if we calculate it with the f_s. That is why it is blind detection no there is no need of f_c. Here f_s and f_c are sampling and carrier frequencies respectively. Determination of carrier frequency is out of scope of this thesis.

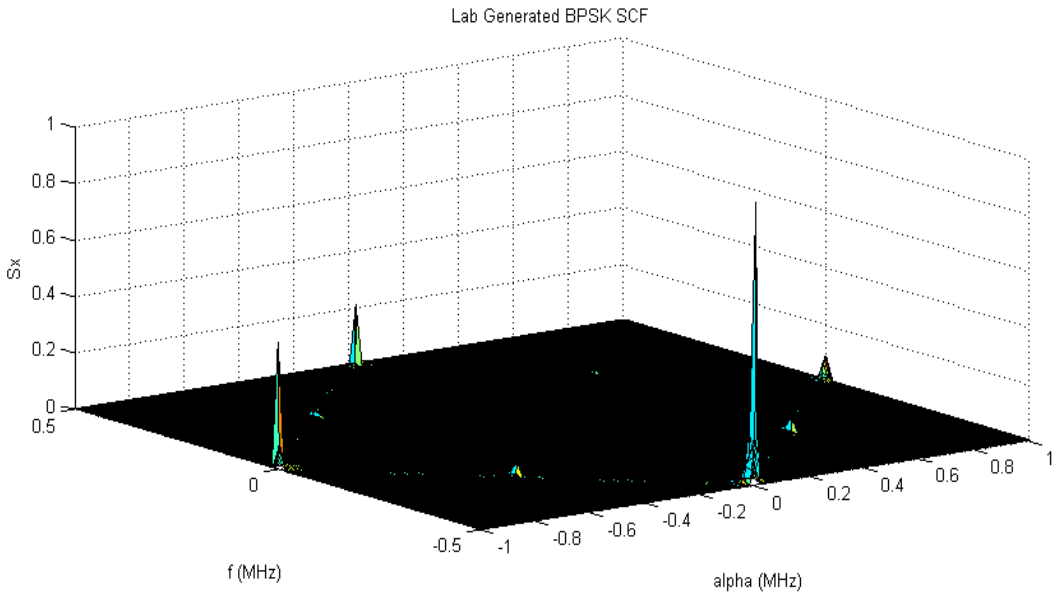

Figure 7-2: The SCF plot of the lab generated BPSK signal

For the shown plot of SCF in Fig.7-2, only a graphical understanding of the features exhibited by BPSK modulated signal (captured through the USRP2) is obtained. Now, the algorithm proposed for detecting these features is based on the hypothesis devised for detecting signal and noise separately in the frequency band under analysis by calculating a normalized vector. Plot of the vector is presented in the Fig. 7-3. The vector points or length is dependent on the resolution of frequency set in the FAM algorithm. Making use of this lower value the proposed technique folds the SCF features and a plot is presented for understanding in Fig. 7-3. The peaks in the plot are the spectral peaks in the SCF. This vector is fairly readable using its indexes by any computer program or hardware solving the problem of extracting SCF features which are well understandable by plotting a 3-dimensional plot.

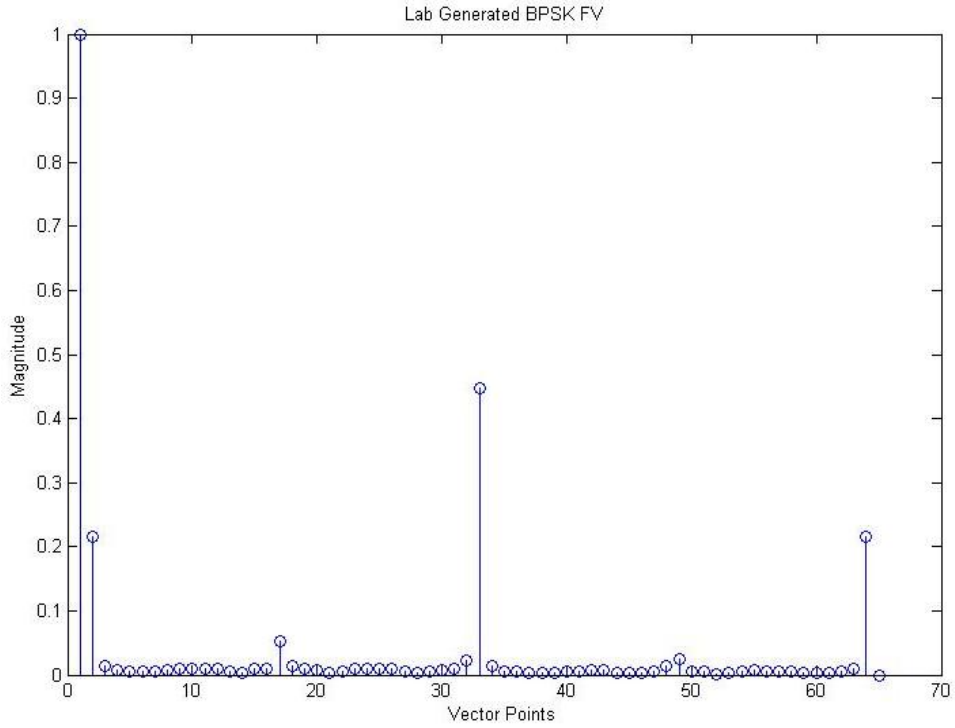

Figure 7-3: Plot of the lab generated BPSK feature vector

One more advantage is that only half of the values can be utilized to detect signal or noise. If the peaks are counted from index 0 to 35, then according to Eq. 5-8 H_1 is true resulting signal detection by the decision block.

7.1.2 QPSK Modulation

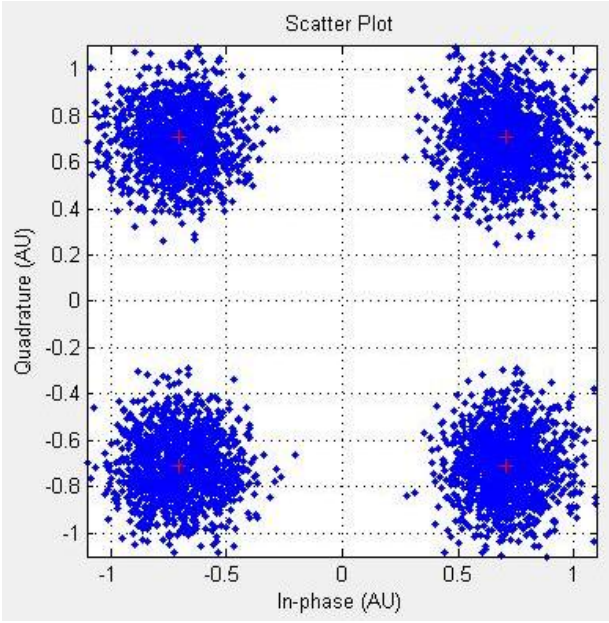

Figure 7-4: Constellation plot of the QPSK sampled data

The QPSK constellation diagram is presented in Fig. 7-4 before applying to the algorithm ensures proper modulation data in the input vector. The SCF plot of Fig. 7-5 has significant peaks at $\alpha = 0$. The ideal SCF should be containing only two peaks at $\alpha = 0$ and no peaks in $f = 0$ axis due to the cancellation of in-phase and quadrature parts [23] but this is only possible when high resolution analysis is done which is computationally complex. Due to the low resolution parameters used with the added advantage of less complex operation, some smaller magnitude peaks are present at the location of $f = 0$.

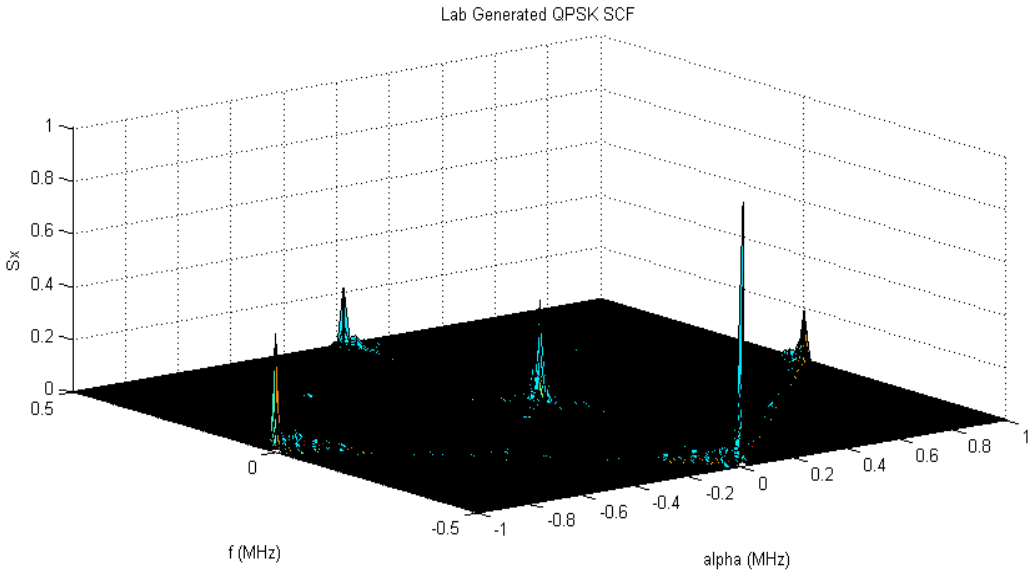

Figure 7-5: SCF Plot of the lab generated QPSK

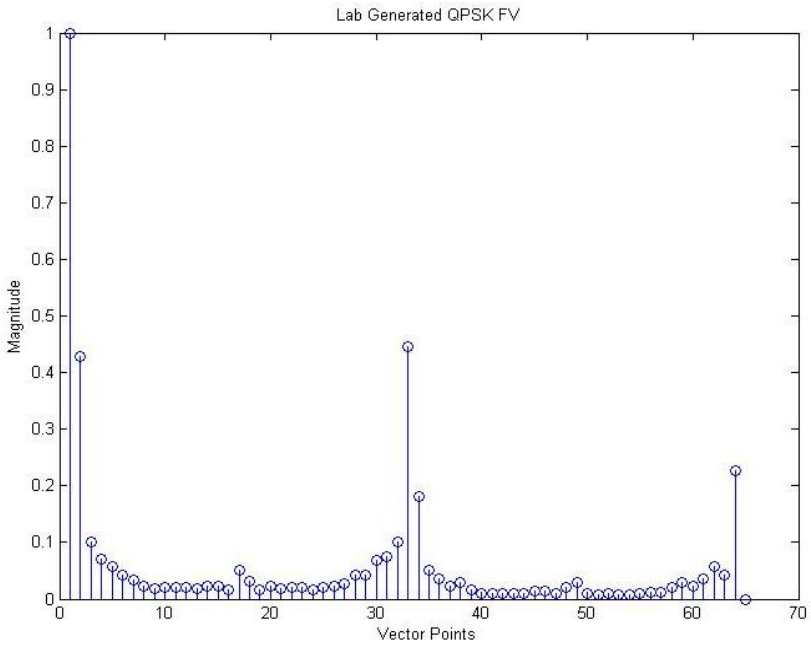

Figure 7-6: Plot of the lab generated QPSK feature vector

This phenomenon does not disturb the detection result. In Fig. 7-6, the calculated vector show peaks which resulted in the detection hypothesis H_1 upon the application of the devised technique. A closer look on the calculated vectors for BPSK and QPSK modulated data highlights the difference of available spectral peaks in the SCF.

7.1.3 16-QAM Modulation

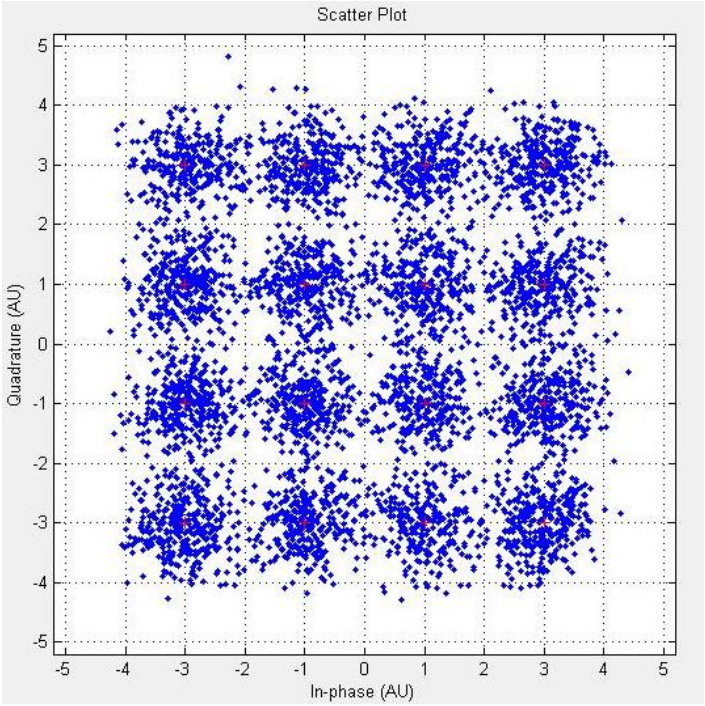

Figure 7-7: Constellation plot of the 16-QAM sampled data

The captured data is first plotted and 16-QAM constellation was obtained in Fig. 7-7. SCF is calculated using the FAM low resolution parameters. 16-QAM is a complex digital modulation. Several peaks are present in Fig. 7-8 at $\alpha = 0$, $\pm 2f_c$ and $f = 0$ axes. This is due to the low resolution analysis resulting in smaller number of cancellations between in-phase and quadrature components. Fig. 7-9, shows the plot of calculated vector containing the significant spectral peaks extracted from 3-dimensional SCF. The detection algorithm when applied resulted in hypothesis H_1 . Since the number of peaks crossing the threshold value $\Upsilon = 0.5$ are less than $\frac{N}{2}$.

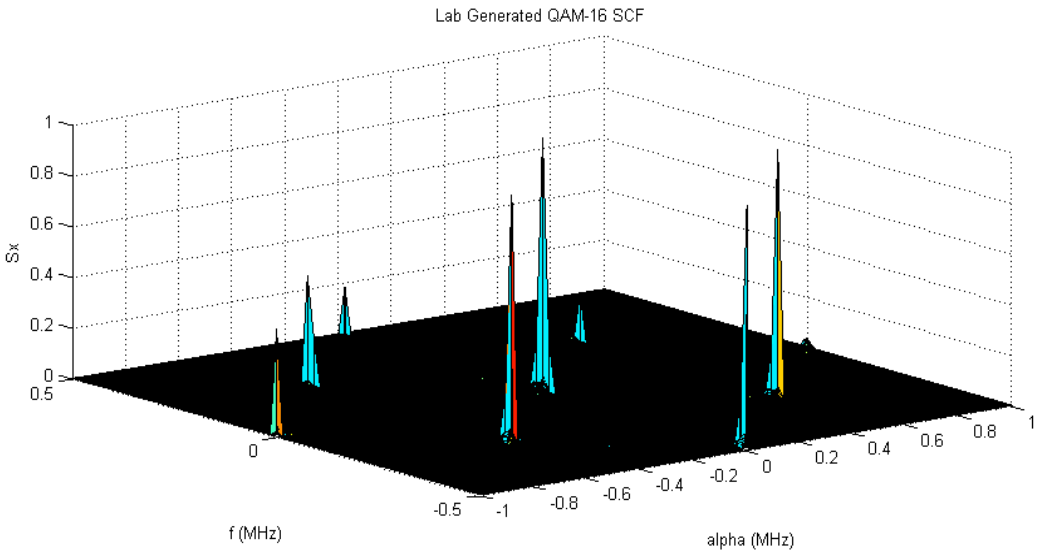

Figure 7-8: SCF plot of the lab generated 16-QAM modulation

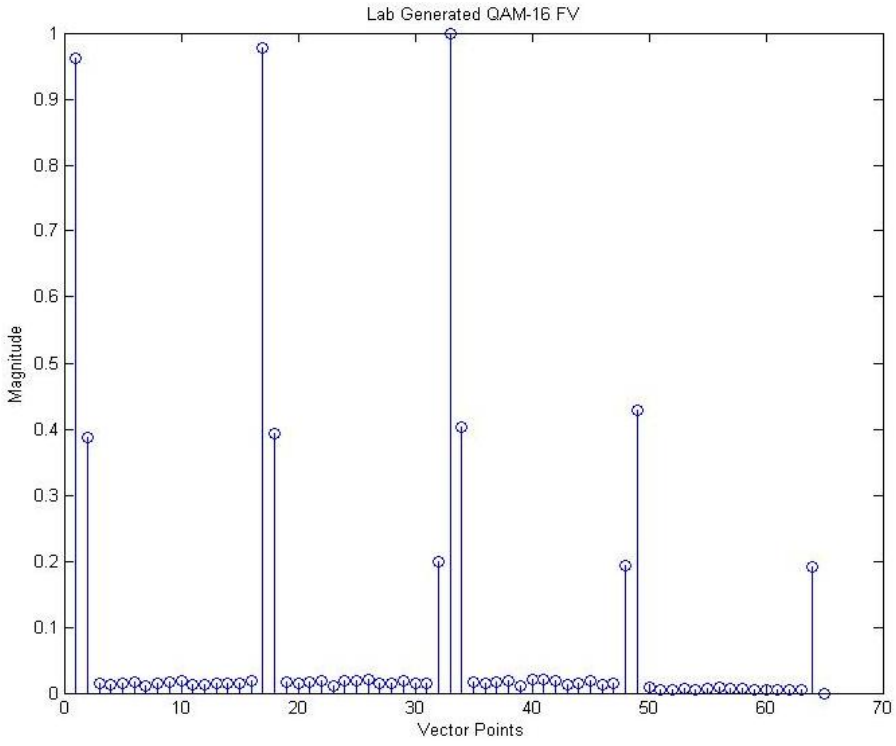

Figure 7-9: Plot of the lab generated 16-QAM feature vector

7.1.4 Noise

SCF plot of noise data as captured through USRP2 is shown in Fig. 7-10. There is no significant spectral peak in the whole SCF except random but symmetric peaky response at α = 0. This is also the power spectral density (PSD) of noise seen in the frequency domain spectrum. According to the basic theory [1], noise exhibits the same particular behaviour as obtained in our analysis that it does not show any feature peaks in its correlation product spectral density. The resultant vector from the detection algorithm is presented in Fig. 7-11. Peaks passing the defined threshold γ are greater than $\frac{N}{2}$ so the detection algorithm will result in H_0. That is no signal present and only noise is detected.

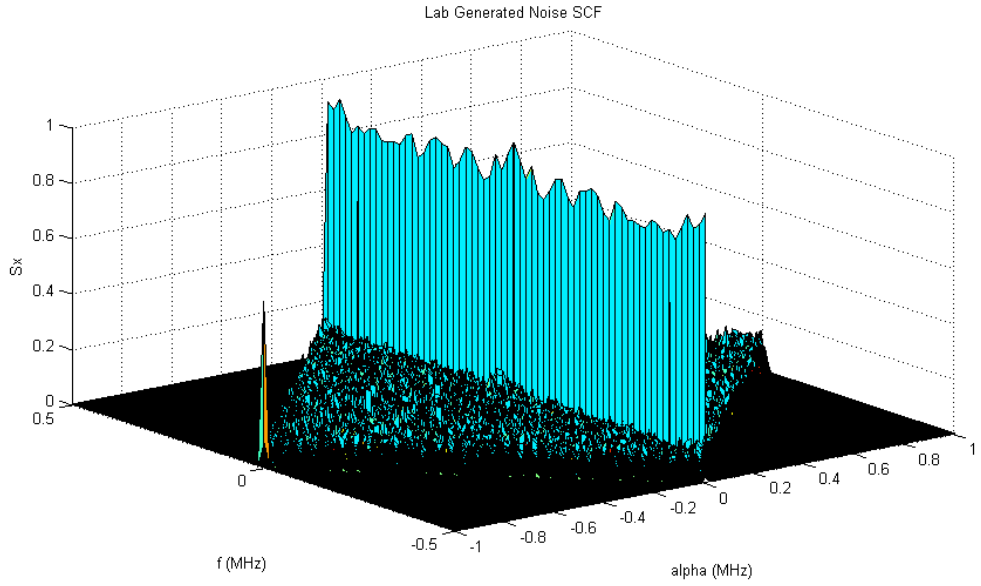

Figure 7-10: SCF plot of the lab generated noise

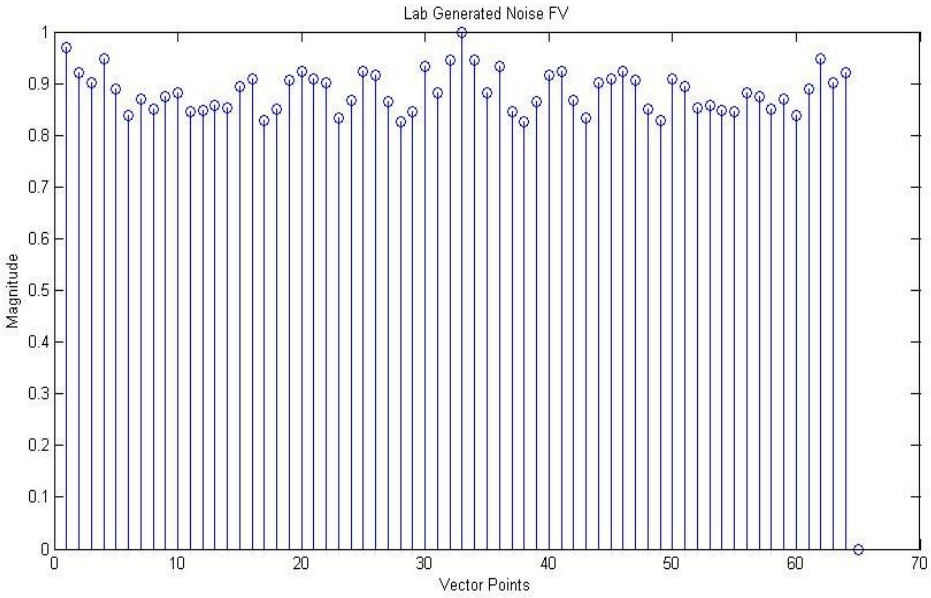

Figure 7-11: Plot of the lab generated noise feature vector

Effect of varying noise variance in the analysed data will have least effect because it is ensured through detailed experimental testing and normalized values are present in the calculated vector and the threshold set for the worst case noise to avoid false detection.

7.2 Real Satellite Signal Approach

In this part of the thesis, the analysis results for the real time satellite signals are being presented. These results were obtained by applying the whole detection algorithm to the captured data from USRP2 connected with a pointed antenna with LNB operating in C-band. The antenna is pointed towards the communication satellite. Proper link was ensured between the antenna and satellite transponder using the connected spectrum analyser. The captured signal spectrum is checked on the spectrum analyser connected using a two port power splitter on which the input signal is the LNB's output and the outputs connected with USRP2 and the spectrum analyser. It is also worth mentioning here that no sort of noise cancellation or conditioning of LNB's output had been carried out before capturing and testing the signals by the detector. The antenna and LNB used in the setup are low-cost off the shelf solution for receive only satellite link. To the best of author's knowledge, the results presented next are one of their kinds since energy detection and only PSD calculations are available so far in the literature addressing the subject of the thesis in the domain of communication satellite signals.

7.2.1 BPSK Modulation

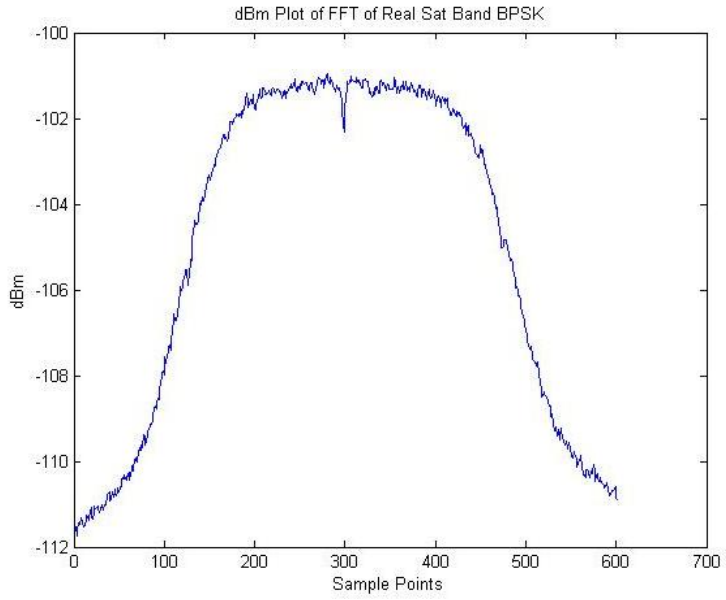

Figure 7-12: FFT plot of the BPSK satellite carrier sampled data

Fig. 7-12 is the plot of magnitude of the FFT in *dBm* units. It is significant to ensure that the sampled data points from USRP2 are having the same BPSK spectrum as of the measured one using the spectrum analyser in experimentation chapter. The SCF plot of Fig. 7-13 is having the features exhibited by the BPSK carrier present in the satellite band. Since, no pre-processing is done to remove the noise effects and corrections to the induced irregularities of LNB's output so SCF is different than that of the SCF of lab generated BPSK and ideal BPSK.

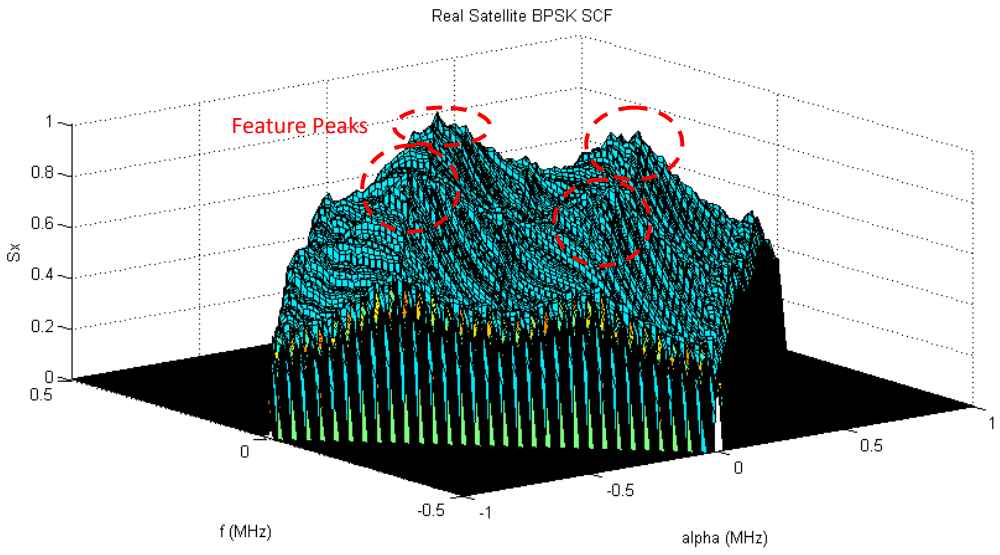

Figure 7-13: SCF plot of real satellite BPSK carrier

The normalized SCF has four bumps two at α = 0 and two at f = 0 axes. These bumps are actually the peaks obtained in the lab generated BPSK SCF. The raised part in the SCF plot represents the noise floor and irregularities induced by the satellite channel and LNB's hardware. It is higher because of lower observation time & frequency resolutions [32]. Discussions of these effects are out of the scope here in this thesis.

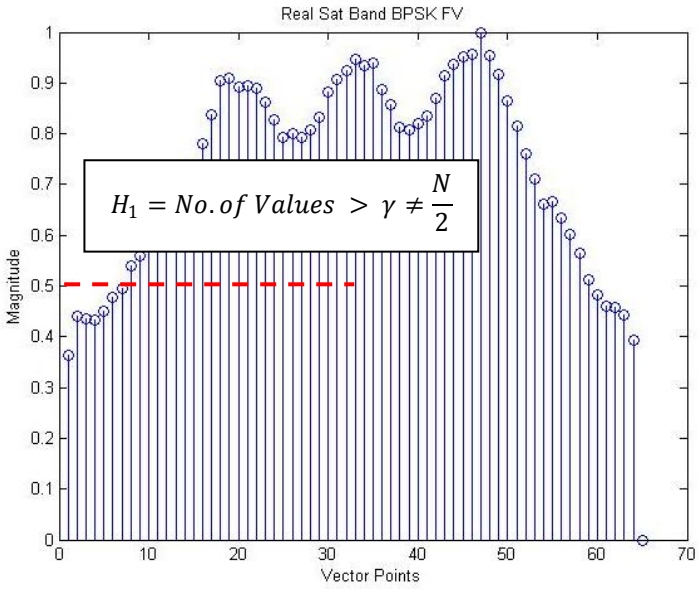

Figure 7-14: Plot of the real satellite BPSK feature vector

Detection algorithm calculates the vector for the SCF presented in Fig. 7-14. The raised noise floor is clearly visible, since the least value in comparison to the lab generated BPSK vector has risen from nearly zero to somewhere near 0.38. The bumps in the SCF can be easily seen in the vector as features of the BPSK signal. The detection block calculates the number of peaks above the threshold of $\Upsilon = 0.5$ for $\frac{N}{2}$ values (where N is the total number of vector points i.e. 70) and results in H_1 hypothesis meaning detection of signal.

7.2.2 QPSK Modulation

Same procedure was repeated for QPSK data samples. First the spectrum plot is obtained from the sample data points as shown in Fig. 7-15 with a close matching with the one measured on the spectrum analyser. The SCF plot shows particular QPSK features disturbed by the noise.

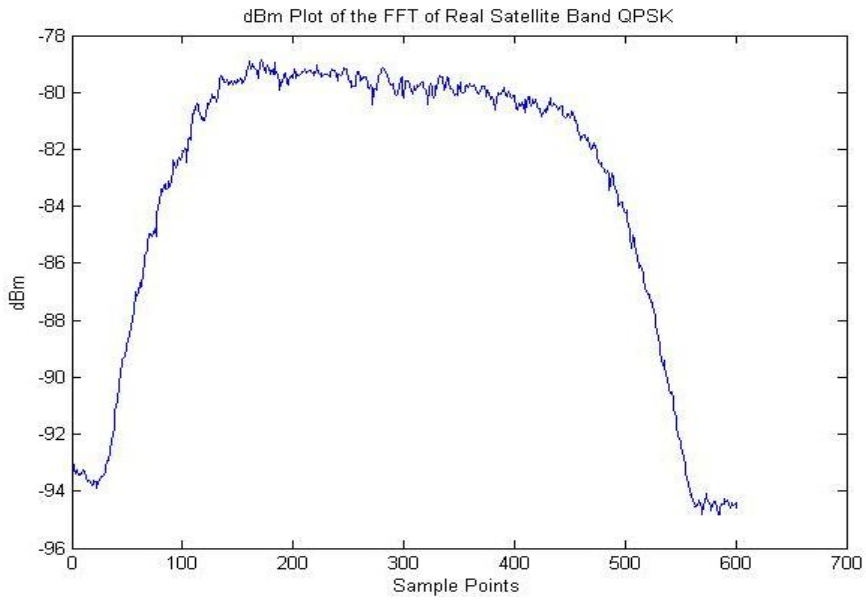

Figure 7-15: FFT plot of the QPSK satellite carrier sampled data

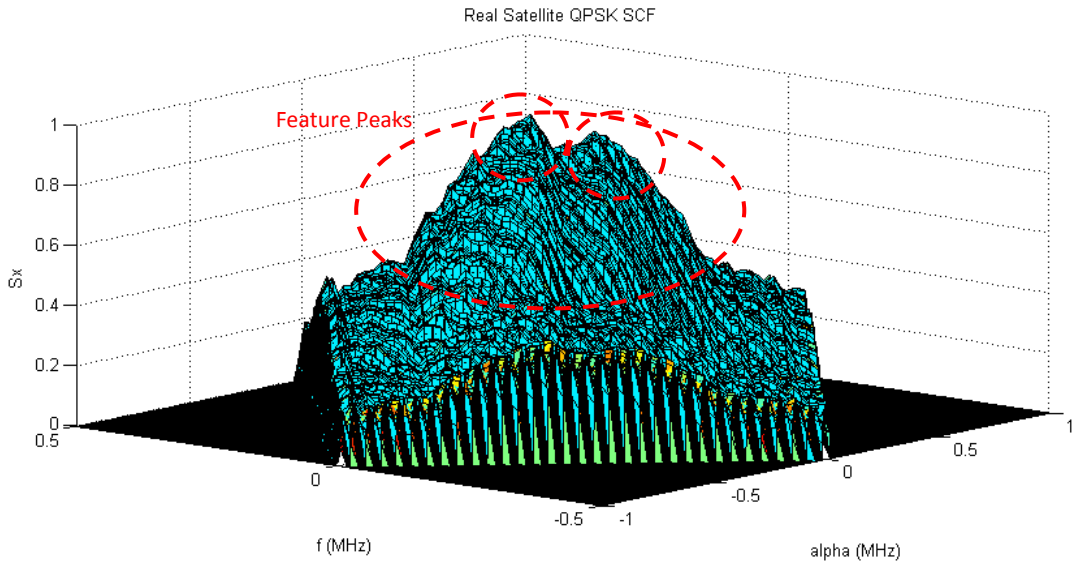

Figure 7-16: SCF plot of the real satellite QPSK carrier

At α = 0 axis, two symmetric raised lobes are present showing the spectral features of QPSK modulation in Fig. 7-16. The raised portion is a bit shifted too because of improper cancellation between in-phase and quadrature portions of the modulated data. But the main concentration is within the area bounded by the $\alpha = 0$ axis.

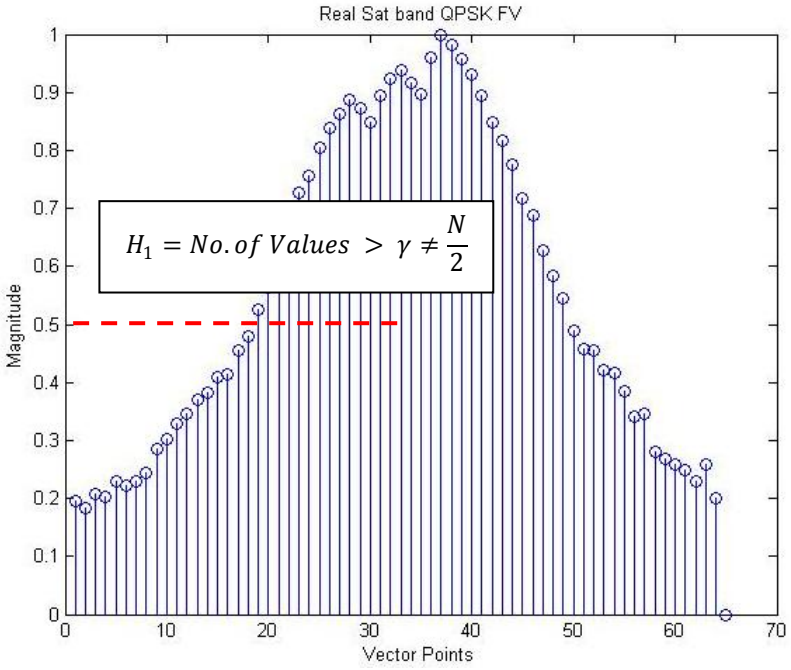

Figure 7-17: Plot of the real satellite QPSK feature vector

The features extracted in the calculated vector for QPSK modulation in Fig. 7-17 are uniquely identifiable. Using the proposed detection algorithm, the values qualifying the set threshold of 0.5 are $< \frac{N}{2}$ so signal is detected and output is H_1.

7.2.3 16-QAM Modulation

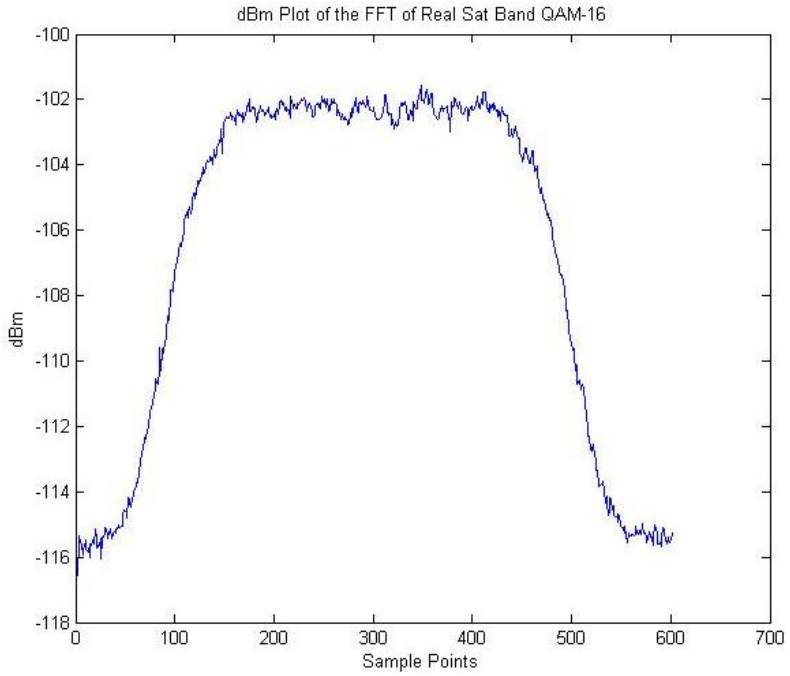

Figure 7-18: FFT plot of the 16-QAM satellite carrier sampled data

Captured data in case of 16-QAM modulation was first ensured by matching the simulated spectrum plot in Fig. 7-18 and that obtained by spectrum analyser presented in the experimentation measured results.

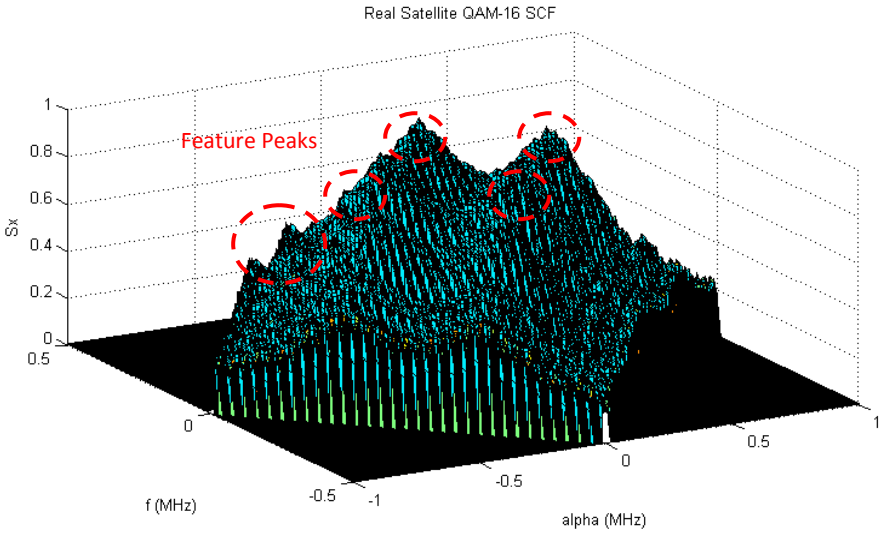

Figure 7-19: SCF plot of real satellite 16-QAM carrier

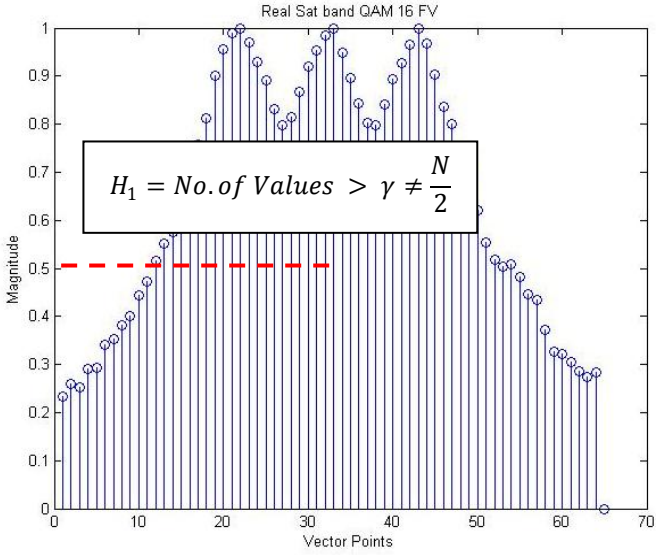

Figure 7-20: Plot of the real satellite 16-QAM feature vector

SCF of 16-QAM carrier in Fig. 7-19 is showing raised lobes at $\alpha = 0$, $\pm 2f_c$ and $f = 0$ locations. These several raised lobes are due to non cancellation of in-phase and quadrature parts of the complex modulation due to low resolution analysis. Extracted vector in Fig. 7-20 satisfies the condition for hypothesis H_1 so detection of signal is resulted by the decision block.

7.2.4 Noise

The spectrum of the captured real-time satellite band noise is shown in Fig. 7-21. The noise spectrum shows rapid power level changes which is significant in processing the noise data because the shown noise spectrum is very far from the usual linear noise floor. The noise PSD presented in the figure below is varying in terms of power levels and this particular noise data set will qualify the threshold set for detecting signal and noise. The analysis of this type of non-linear noise floor with the proposed technique is presented for testing it under hypothesis H_0.

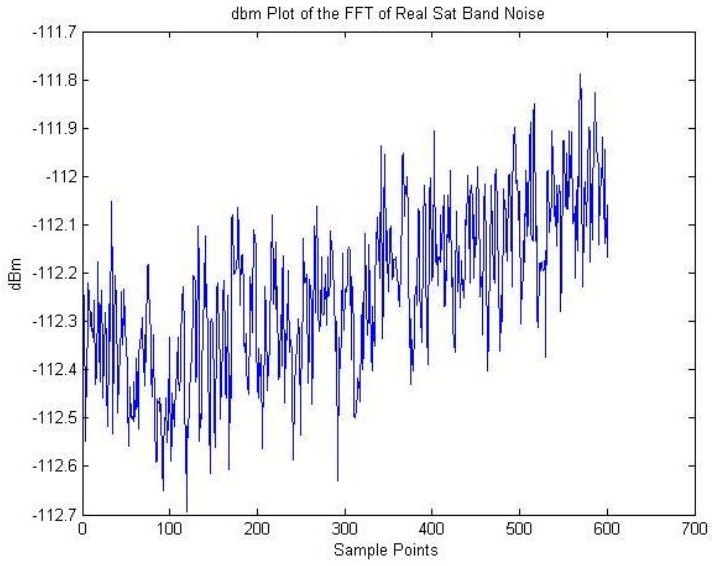

Figure 7-21: FFT plot of the real satellite noise sampled data

No particular spectral peaks are shown in the SCF of noise in the satellite frequency band. In Fig. 7-22, the SCF for idle frequency location where there is no transmission going on is presented. In the whole SCF no particular pattern is available. Since, all the captured I & Q samples are same so SCF has the same spectral values in the bi-frequency plane. This is the reason for a raised noise bed in the SCF.

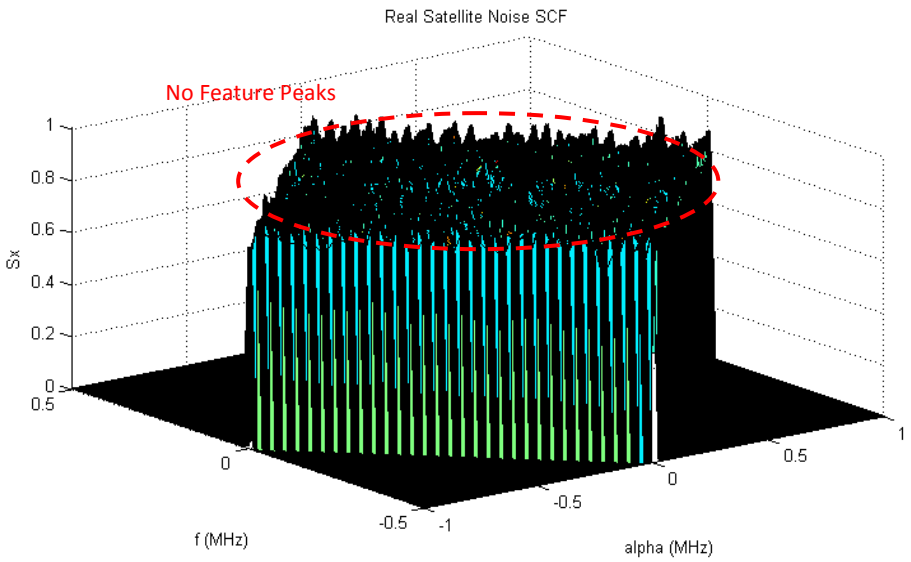

Figure 7-22: SCF plot of the real satellite band noise

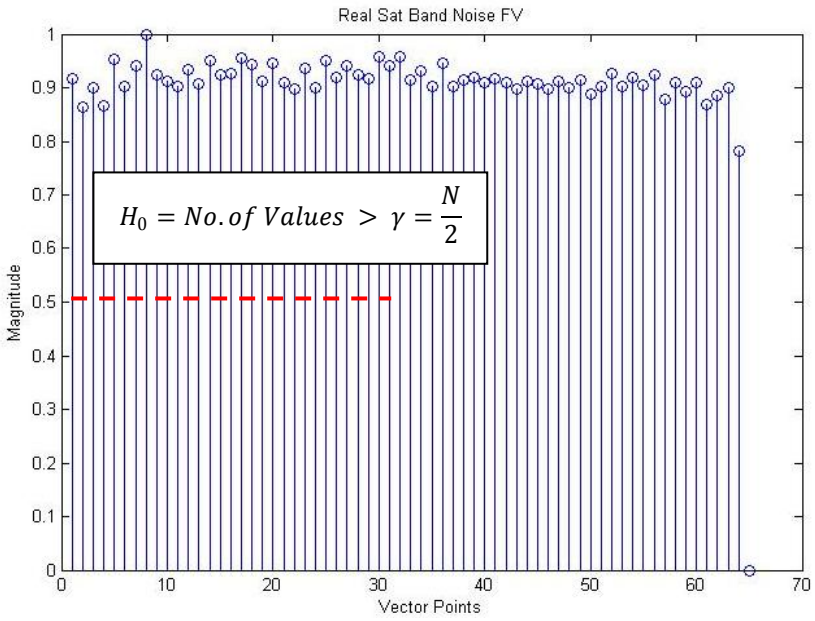

Figure 7-23: Plot of the real satellite noise feature vector

Fig. 7-23 shows the calculated vector according to the proposed detection scheme from the noise SCF. All the $\frac{N}{2}$ values are passing the threshold value of 0.5 in the calculated feature vector so hypothesis H_0 is resulted by the decision block sensing an idle frequency channel equals to half the bandwidth of the sampling frequency.

So far, the detection of BPSK, QPSK and 16-QAM carriers captured in the satellite band as signals in general has been presented. The algorithm then further applies fourth order cumulnats as statistical classification tool for modulation type in the detected signal.

Particular values of cumulants obtained for different modulation types can assure the simple classification of the detected signal.

7.3 Modulation Classification Using Cumulants on Calculated Vector

Cumulant	BPSK	QPSK	16-QAM	Noise
	Values for Calculated Vector (Real Satellite Signals)			
$\widehat{C40}$	*-1.03995*	*-0.50965*	*-0.38224*	*-1.29625*
$\widehat{C42}$	*-1.03995*	*-0.50965*	*-0.38224*	*-1.29625*

Table 4 : Fourth order- Cumulant values of feature vector

For real constellation cumulants values follows $C_{20} = C_{21}$ and $C_{40} = C_{42}$ [24]. This validates the results obtained through simulations for cumulants for different modulations and noise. The classifier in the algorithm compares the incoming value with the look up table of the values in Table 4. The classification of modulation decision takes place with the result of comparison of the incoming value and the present values obtained through testing the statistics of cumulants obtained for noise and modulations. If the incoming value does not lie in the ranges presented, the classifier results in un-known modulation.

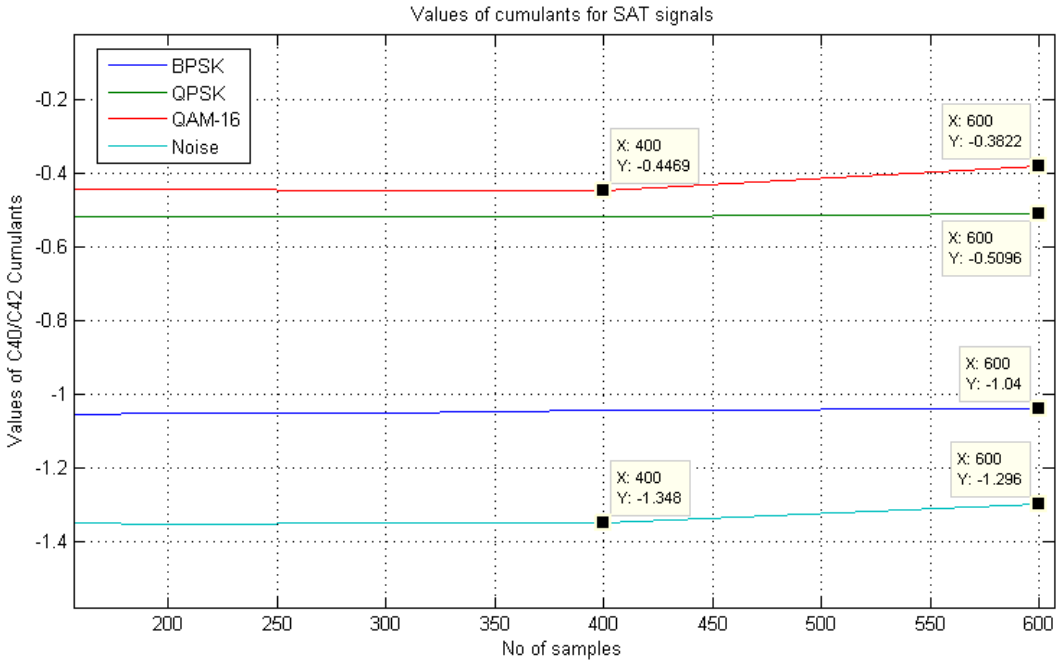

Figure 7-24: Cumulant values for BPSK, QPSK, 16-QAM and Noise Data

A plot of cumulant values for different modulations and noisy data obtained through the algorithm is shown in Fig. 7-24. Values for modulated data from the real time satellite sampled data are present. To clarify the values of Table 4, different values obtained for BPSK, QPSK, 16-QAM and noise data by using the cumulant calculations are present in the plot of the figure. The shown values in the plot are being used by the classification block of the algorithm to differentiate between different modulations. The input data from which these values were obtained was that of the column vector Vi from Eq. 5-4.

7.4 Trend Analysis of Cumulant Values Obtained

The values of cumulants obtained as listed in Table 4 shows the same trend as the HOS analysis on the complex valued signals. The modulation formats of BPSK, QPSK and 16-QAM have shown approximately half of the values obtained by HOS cumulants applied on the complex signal samples. The values from [24] for the modulation formats are *BPSK= -2.0000, QPSK = -1.0000 and 16-QAM = -0.6047*. The trend shows that as the modulation gets more complex and dense the cumulant values become smaller. The reason for this trend lies in the definition of cumulants. Since, the fourth order cumulants are dependent on the second order statistics values C_{20} and C_{21} [24]-[25]. For denser modulations, the sum of these statistical values becomes smaller due to correlation values and cancellations of I & Q parts whether completely or partially. Fig. 7-24 shows the trend of values obtained using cumulants for different sample sizes on the calculated feature vector obtained from the proposed technique. Remember that the feature vector contains the magnitudes FFT values of feature peaks and has only a total of 65 values which is far smaller than the sample sizes on which cumulants were calculated in [24] & [33]. So, the trend of approximately half values as compared to the theoretical values in literature is due to the lower sample size and magnitudes. Secondly, only feature values have been used in calculating cumulants. It has significantly reduced the computational complexity of the cumulant calculations and the pattern for modulations is in a great logical agreement with the theoretical pattern. The obtained values of cumulants with respect to the changing sample sizes (input to FAM from where the SCF containing the feature peaks is calculated and then feature vector is extracted) are showing lesser amount of variations. Due to normalized SCF and fixed parameters for the sample size and FAM the cumulant values obtained are consistent. The values are unique forming the same pattern as the theory suggests for the modulation formats under considerations. Noise has different and greatest value than that of the three modulations.

These values are used by the classifier to decide about the type of the detected signal or noise successfully.

7.5 Comparative Analysis

In order to emphasis the valuable contributions of the discussed technique for detection of satellite signals and its classification capability, comparative analysis with other state-of-the-art techniques built in the literature has been carried out. The cyclic spectral density resulting from cyclostationary analysis has different built-in statistical properties which are usually utilize by signal detectors specially, the symmetric property of the SCF is used. This works by checking the equality of the feature peak magnitudes at specific locations in bi-frequency SCF on cyclic frequency axis [19] & [20]. For this equality decision by measuring the magnitude at symmetric SCF location, high resolution analysis is done which introduces high complexity and computational time. In the proposed research, the objective was to achieve such a detection technique which works with low resolution frequency parameters, least affected by the magnitudes of the peaks (when using low resolutions peak's magnitude attenuates), works blindly (without any prior knowledge of the signal under consideration) and should extract feature peaks form the SCF bi-frequency two variable function in a simple way. The feature vector extracted has the least possible index and values reducing post SCF calculations. Despite being less complex, the calculated SCF contains all the features exhibited by the modulations (BPSK, QPSK and 16-QAM) as the theory suggests. The results from this work and other laid out techniques can be compared on the following grounds.

7.5.1 High Cyclic Frequency Resolution

In [44], a novel modulation detection technique has been presented for detecting acoustic signals using cyclostationary analysis. The technique works by calculating SCF at dynamic cyclic resolutions. For specific locations of cyclic frequency as a function of the carrier frequency, high resolution SCF as in Table 5 is calculated and for the rest of the bi-frequency plane low resolution calculations are done see Fig. 7-25 (a). For signal detection decision ratio of the peaks in frequency and cyclic frequency axes is calculated. The author claims reduction in complexity by observing and analysing short duration signals for SCF but in Fig. 7-25 (b), the SCF misses the significant peaks at $\alpha = 2F_c$ for BPSK modulation when a little shift in F_c and a low $\Delta\alpha$ is used. This leads to false detection of modulation. The values for cyclic frequency resolutions are presented in Table 5. For the technique in [44], SCF is

calculated with high and low resolutions imposing computational complexities while for the proposed technique in this research works well with low resolution cyclic frequency value.

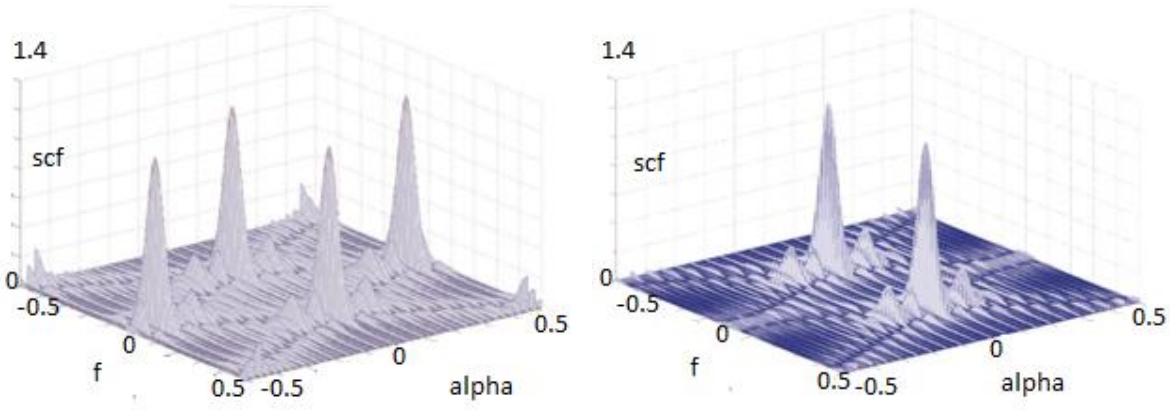

(a) (b)

Figure 7-25: (a) SCF of BPSK, Fc=17000, Fb=4000, Fs=80000, dalpha=0.005 (Fig.4 [44]),

(b) SCF of BPSK, Fc=17020, Fb=4000, Fs=80000, dalpha=0.001 (Fig. 5 [44])

Δα (Dynamic SCF in [44])	**Δα (Proposed Technique)**
$5x10^{-5}$*(High Resolution SCF)* + $1x10^{-2}$*(Low Resolution SCF)*	$2x10^{-4}$ *(Low Resolution SCF)*

Table 5: Cyclic frequency resolutions of [44] vs. Proposed technique

7.5.2 FAM Complexity and Computational Time

N(samples)	N'	**L**	**P**	**Resolution (Hz)**	**Time (s)**
2^{18}	2^8	2^6	2^{12}	2^6	60.0
2^{17}	2^8	2^6	2^{11}	2^7	30.55
2^{16}	2^8	2^6	2^{10}	2^8	13.28
2^{15}	2^7	2^5	2^{10}	2^9	3.39
2^{14}	2^6	2^4	2^{10}	2^{10}	0.896
2^{13}	2^5	2^3	2^{10}	2^{11}	0.273
2^{10}	2^6	2^4	2^5	2^{11}	0.1059

Table 6: FAM computing time and parameters in (Table 1 of [12]) vs. Proposed technique

For calculating the SCF, time smoothing FAM algorithm has been used in the proposed detection technique for estimating the features of the detecting signal. In Table 6, the parameters of FAM with their computing time have been listed. These parameters are mainly dependent upon the number of samples used and the resolution of frequency selected. These values have been taken from [12] and since the computing time is based on the platform so

same platform (Intel Core2 Duo 2.54 GHz with 2GB RAM) as mentioned in [12] has been used to calculated the computing time and FAM a parameters of the proposed technique boxed in red as the last entry in the table. It can be concluded that comparatively the proposed detection technique has lesser number of samples and least computing time.

7.5.3 Wavelet Based Technique

For wide band cyclostationary analysis, one of the techniques for detection of peaks in the calculated SCF is by using Wavelets [39]. Wavelets are applied to SCF considering it as a 2-dimensional grey image. The application of wavelets significantly removes noise in the SCF introduced due to compressed sensing and helped in producing improved SCF plots. The technique comes with SCF matrix calculations using compressed sensing convex reconstruction algorithm and then it calculates the wavelet coefficients, edge magnitudes and gradients of the peaky features to remove noise and results in a de-noised SCF as shown in Fig. 7-26 (b).

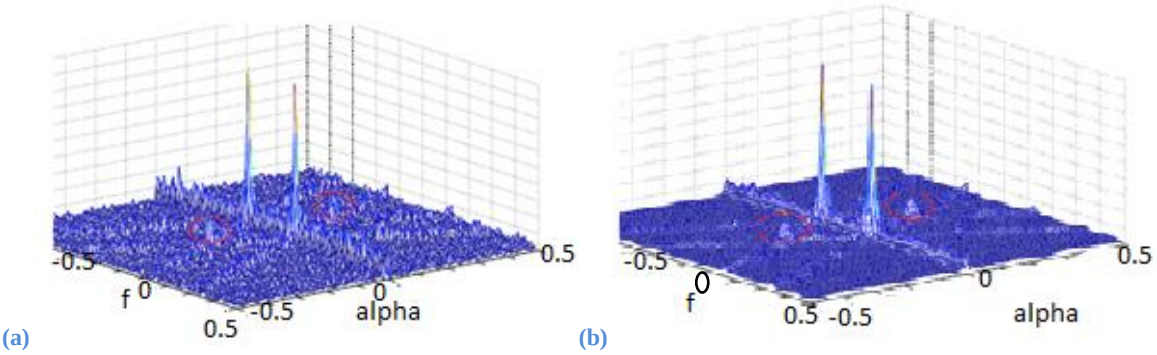

Figure 7-26: (a) Before the Noise Reduction at SNR=-5dB, (b) After the Noise Reduction (Fig.2 of [39]),

In comparison to the proposed technique of this research, the detection probability is very high in case of signal SNR = -5dB. This is because of the detection algorithm design strategy and its independence with the noise statistics due to normalized feature's magnitudes. Also, the computational complexities of wavelets are avoided in the technique.

7.5.4 ANN Based Modulation Recognition

In [40], cyclostationary analysis has been utilized to classify the modulation format of the signal. The extracted features from the signal are in terms of coherence function and cyclic domain profile as can be seen in Fig. 7-27. The classifier used to actually perform the classification decision is an artificial neural network (ANN). Classifier needs training data in large quantities as a prerequisite. Using delta rule (errors calculated and compared between

desired and obtained outputs) training of ANN is carried out. The SOF (coherence function) and cyclic domain profile (CDP) requires estimation of the spectral density first. The iterative algorithm is feed forward back propagation algorithm (FFBPA) details of which are presented in [40].

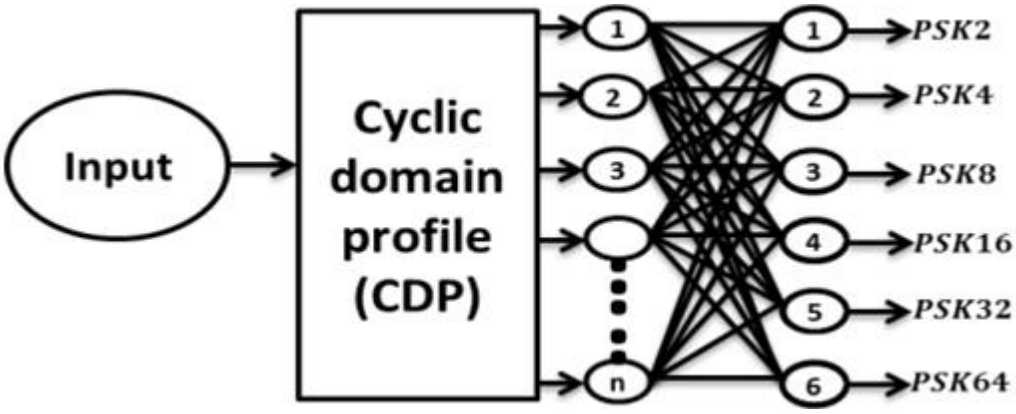

Figure 7-27: Proposed algorithm for classification of PSK modulation formats (Fig.8 [40]),

Overall, in comparison to the proposed technique of cumulant based classification, the former is quite simpler and low on computation than ANN based classification. However, the classification method has a very high classification probability at SNR = 0 dB but, a large computation and signal processing is involved in calculating SCF, SOF & CDP and then ANN (FFBPA) classification.

7.5.5 Single cyclic frequency techniques

In [19], a novel technique for signal detection using CAF symmetry test is presented. It is using orthogonal matching point (OMP) algorithm to estimate the CAF of the signal and then check for symmetric feature of the signals at certain α. In comparison to the proposed algorithm, it is an iterative algorithm with high resolution discrete fourier transform (DFT). This makes it more time consuming and complex due to iterations, number of DFT and IDFT operations. A real-time CAF symmetry check algorithm for signal detection is presented in [20]. It is also using OMP algorithm and then check for the feature peak magnitude value in CAF at α & -α. The probability of detection at SNR= -15 dB is $P_d < 0.2$ which is in the proposed technique is $P_d = 0.9$. Also, the FFT size of 2048 has been used in the said technique which is just 32 in our case as the first FFT size in FAM. [23] has an alternate to FAM technique (details are in literature review) but it has complexity of two FFTs and one IFFT to reach to the detection decision when compared to the proposed technique. Also the probability of detection in lower SNR is almost the same for both the techniques.

The performance in terms of detection probability, computational cost and execution time for the proposed technique is laid down in the next chapter.

Chapter 8. **Performance Analysis**

The performance analysis of the spectrum sensing technique is given by the two major factors as in [2]. One of the major factors is the probability of detection of the proposed technique in changing SNR conditions. Probability of detection (P_d) shows how correctly the proposed algorithm can detect a signal in the lower and higher SNR conditions. There are certain methods and experimentations [2, 17 & 29] including Monte Carlo simulations or custom experiment designed to calculate the probability of detection. The lowest possible probability of false alarm is selected to perform these experiments. In our case, we have set probability of false alarm (P_f) to be 0.01. The probability of detection versus SNR plot has been carried out by applying the conventional definition of probability calculation. The probability is calculated in a random experiment of 27 trials for each modulation format (BPSK, QPSK, and 16-QAM). Signal detection is done under SNR set of $SNR\ \epsilon\ [-20, -15, 10, -5, 0, 5, 10, 15]$. The second most important parameter is the complexity analysis of the technique. It is presented next. The complexity of the technique in terms of the calculation and operational resources comes out to be equal to the complexity of FAM algorithm with low resolution analysis than in [5] & [12] due to larger α and f resolutions.

8.1 Probability of Detection

For performance analysis of the detection technique in low SNR, probability detection experimentation is carried out [2]. The detection technique shows excellent performance under low SNR condition. For typical SNR range of establishing a communication link in satellite (SNR values between 5dB to 20dB), the probability of detecting the signal is approximately 100% within the defined threshold statistics. In Fig. 8-1, the trend shows lowest probability of detection at SNR = -20dB. This is due to the fact that at -20dB SNR the peaks in the calculated vector by the proposed technique are well above the defined threshold of 0.5 due to increased noise floor than signal. So detection is disturbed and probability of false alarm is increased. For SNR above -20dB, signal is detected with good probability of detection with a maximum probability of false alarm of 0.1.

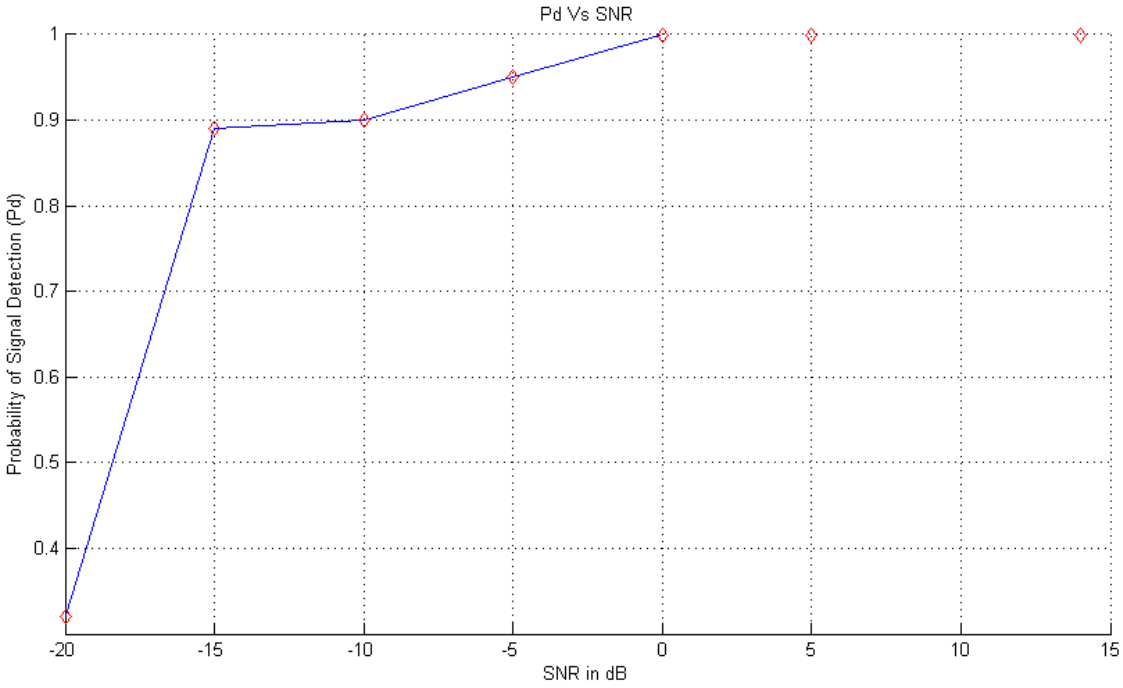

Figure 8-1: Probability of Detection vs. SNR Plot

8.2 Computational Complexity Analysis

The calculation of Cyclostationary features of modulated signals is a computational hungry task. It was considered to be complex in computing the SCF estimates for complex signals [1]. In this research, FAM method has been used which is an efficient time smoothing method for the calculation of the estimates of SCF [1]. Although, it is an efficient calculation algorithm for SCF, but it includes the computation of windowing, complex demodulates calculations and above all the FFT operations are dominant in the FAM computational complexity [5, 12] & [34]-[35]. The complexity of SCF for estimating the features using FAM is $O\left(\frac{NN'}{L}\left(log_2 N' + N' log_2(\frac{N}{L})\right)\right)$. Where N, N′ and L represents the parameters in FAM algorithm naming number of samples, number of samples to calculate complex demodulates and decimation factor for channelization of input respectively [12]. Main benefit of the proposed detection technique is that it works for low resolution analysis. Low resolution analysis reduces the values of the above parameters of FAM by using larger values of Δα and Δf. Complexity of the feature vector calculations of the detection technique and cumulants based classification has calculation complexity of $O(0.5M + 4N)$ [24]. Additionally, the technique is computationally less complex since there are no covariance matrix calculations. Also, only $\frac{M}{2}$ vector points are used from the SCF to detect the signals as

in [18]. Values of N, N' and L depends upon the resolution of frequency and cyclic frequency parameters of the FAM algorithm. In Table 5, different resolutions of cyclic frequency and the coarse frequency values are presented. The smaller the values of these resolutions, greater the number of samples and in turn higher the number of complex operations required to be performed on the hardware for FAM algorithm are required. The values used in this work are enclosed in the highlighted red rectangle in Table 5. The complex operations required are least among the listed values in the table. From the results and performance analysis it is ensured that SCF features, detection of signal, its classification using cumulants and less complex numerical computations have been done by the proposed research using low resolution parameters for FAM. The numbers of operation by FAM are the least in which spectrum sensing in its true nature has been carried out.

Δf	$\Delta\alpha$	N	N'	L	O
200000	20000	512	64	16	667648
20000	2000	8192	512	128	100958208
2000	480	32768	8192	2048	4.2967e+09
2000	200	65536	8192	2048	1.0741e+10
2000	50	262144	8192	2048	6.0143e+10

Table 7: Values of complex operations required by the number of samples on different resolutions

As far as the time taken by the execution of algorithm is concerned, according to [12] it is dependent on the values of N the number of samples to be processed by the FAM. From the aspect of hardware setup, the running USRP2 output to the algorithm containing a large buffered data does not affect the time taken to process it because numbers of samples are defined by the set frequency and cyclic frequency resolutions Δf and $\Delta\alpha$ which defines the number of samples. The plot of Fig. 8-2 shows little change in time taken by FAM with increasing number of samples input from the USRP2 captured file. Only N samples are processed for calculating the SCF of the given input data from USRP2 for the set resolutions highlighted in Table 5. So, real-time operation will take the same execution time for the specified platform as mentioned in experimentation chapter which is the lowest possible time using the resolution parameters and number of samples. It is therefore has least effect of USRP2 increasing number of samples on execution time. But, at-least N number of sample points i.e. $N = 512$ must be provided by the hardware so that features of SCF can be calculated effectively.

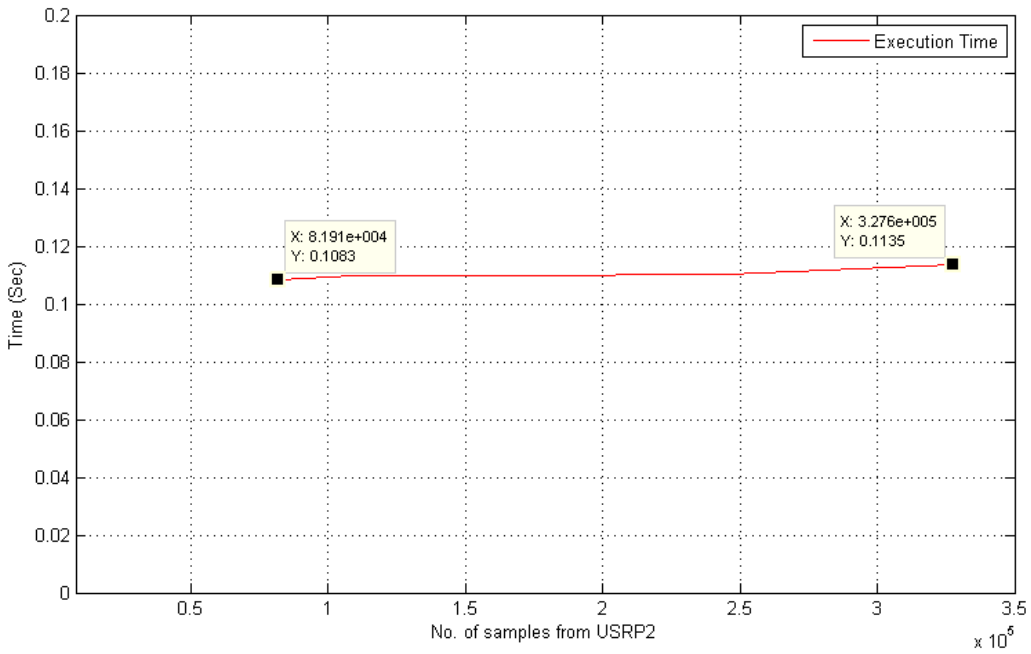

Figure 8-2: Execution time of FAM for number of USRP2 samples

The captured file from GNU Radio flowgraph containing the USRP2 samples of the data is processed by the algorithm in Matlab. Time for capturing the samples from the hardware was *5* seconds in which a total of *327642* samples were captured and saved in a file using the flow graph. The platform specific elapsed time was determined by 'tic and toc' commands of Matlab. Different indexes of the input vector (read from the captured file in Matlab) were used and execution elapsed time was calculated. In Fig. 8-2 it is evident that there is a little change in the execution time with increasing number of captured samples because the FAM algorithm uses only N number of samples which is 512 for the set frequency resolutions in this work. Thus, the proposed algorithm works with low resolution, less complexity and least time consumption, ensuring required features in the SCF.

In the next chapter, concluding remarks and prospective future work is presented. There is a lot of potential in the area of spectrum sensing. Detection algorithms and its application to the signals are not only limited to one domain but has a vast scope in engineering sciences.

Chapter 9. **Conclusion and Future Work**

9.1 Conclusion

In this research cyclostationary analysis of real time satellite signals with efficient FAM algorithm using low resolution parameters for faster execution have been presented. SCF features of real time satellite carriers are presented and a unique, less complex and simple technique for detecting signal or noise is devised. The proposed technique blindly works for BPSK, QPSK and 16-QAM modulated carriers of satellite with minimal user interaction. Also no knowledge of the interfering noise power level is required in the detection phase. This new technique works with the modern SDR based cognitive radio platform front-end (USRP2) so it can be utilized in evolving satellite cognitive radio designs for the purpose of spectrum sensing. For conventional techniques, magnitude, variance and exact location of the feature peaks are very critical. This criticality has been reduced in the proposed technique by maximum value normalization as in [14] and no dependence upon exact locations for cyclic frequency and frequency axes. Also for this technique to work only some of the feature peaks are required without any restriction of their location of occurrence. Significantly, with the processing point of view, the detector is able to work at low resolution parameters for frequency f and cyclic frequency α. Using said parameters least number of complex operations is achieved with significant features in the SCF. Only $\frac{N}{2}$ points are used to detect the presence of signal in the calculated feature vector of length N which reduces the complexity as in [18]. The probability of detection in lower SNR conditions is also satisfactory for the proposed technique. Further, for the classification of the modulated signals after being detected by the spectrum sensing algorithm is done using fourth order cumulants. Successive ranges for BPSK, QPSK and 16-QAM modulated carriers of satellite and lab generated signals has been achieved. With this classification capability, identification and validation of an authentic primary carrier can be done by the secondary user or any government agency. The novel application is that Cumulants were calculated on the real feature vector values extracted from the calculated SCF instead of applying them to the complex I & Q samples of the signal under analysis. It significantly reduces the calculation complexity in comparison with the conventional cumulant calculations considering the signal $y(t)$. Comparative analysis with conventional techniques revealed that this new spectrum sensing algorithm forms good connection with the background theory and shows good bond with the theoretical results.

9.2 Future work

As a future perspective, the whole algorithm can be implemented using C++ programming language and with python wrappers it can be directly implemented as a new block in GNURADIO. In this way, a real time spectrum sensing system can be demonstrated for satellite cognitive radios. The cumulant based classification provides a simpler way to identify the modulation type of the primary signal present in the channel. This classification capability enables the cognitive spectrum sensing engine to monitor the channel and validate the authenticity of the detected signal. This can be used in a manner that if the modulation type comes out to be different than known for the primary user in a specific channel, it can be reported for certain necessary actions to prevent the unauthorized use of the spectrum. Certain industry practices of suppression of such an unauthorised carrier can be carried out by the relevant satellite operator upon being reported by the secondary user utilizing the spectrum sensing engine proposed in this research.

References

[1] W. A. Gardner, “Cyclostationarity in Communications and Signal Processing”, Ed. W. A. Gardner. *IEEE Press*, New York, 1994.

[2] P. D. Sutton, K. E. Nolan, and L. E. Doyle, "Cyclostationary signatures in practical cognitive radio applications," *IEEE Journal on Selected Areas in Communications*, vol. 26, no. 1, pp. 13-24, 2008.

[3] J. Mitola IIIand G. Maguire Jr "Cognitive Radio: Making Software Radios More Personal", *IEEE Pers. Commun.*, vol. 6, no. 4, pp.13 -18 1999

[4] D.Tarchi, A.Guidotti, V.Icolari, A.Varelli-Coralli, S.K. Sharma, S.Chatzinotas, S.Maleki, B.Evans, P.Thompson, W.Tang, J.Grotz, “Technical Challenges for Cognitive Radio Application in Satellite Communications”, *9th International Conference on Cognitive Radio Oriented Wireless Networks (CROWNCOM)*, 2014

[5] E. Rebeiz and D. Cabric, "Blind modulation classification based on spectral correlation and its robustness to timing mismatch," *Military Communications Conference*, 2011, pp. 277-282

[6] R. Zhou, X. Li, T. Yang, Z. Liu and Z. Wu, "Real-time Cyclostationary Analysis for Cognitive Radio via Software Defined Radio," *IEEE Globe-com,* 2012.

[7] T. Yucek and H. Arslan, “A survey of spectrum sensing algorithms for cognitive radio applications,” *IEEE Communications Surveys Tutorials*, vol. 11, no. 1, First 2009.

[8] E. Like, V. Chakravarthy, P. Ratazzi and Z. Wu, “Signal Classification in Fading Channels Using Cyclic Spectral Analysis”, *EURASIP J. Wirel. Commun. Netw*, vol. 2009, no. 1, p. 879812, 2009.

[9] B. E. Guenther, “Multi-User Signal Classification via Cyclic Spectral Analysis”, Master Thesis, Wright State University, USA, 2009.

[10] R. Roberts, W. Brown, and H. Loomis, “Computationally Efficient Algorithms for Cyclic Spectral Analysis”, *Signal Processing Magazine, IEEE,* vol. 8, no. 2, pp. 38-49, 1991.

[11] W.A. Brown, and H. H. Loomis, “Digital Implementations of Spectral Correlation Analyzers”, *IEEE Transactions on signal processing*, vol. 41, no. 2, Febru-ary 1993.

[12] F. Ge and C.W. Bostian, "A Parallel Computing Based Spectrum Sensing Approach for Signal Detection under Conditions of Low SNR and Rayleigh Multipath Fading," *Proc. the 3rd IEEE Symposium on New Frontiers in Dynamic Spectrum Access Networks*, pp. 1-10, Oct. 2008.

[13] F. Paisana, N. Prasad, A. Rodrigues, and R. Prasad, "An alternative implementation of a cyclostationary detector," *Wireless Personal Multimedia Communications (WPMC), 2012 15th International Symposium on, 2012*

[14] J.Renard, L.Lampe & F. Horlin, “Nonparametric Cyclic Polyspectrum-Based Spectrum Sensing”, *IEEE Wireless Communications Letters, Vol. 2, No. 1, February 2013.*

[15] G. Baldini, R. Guiliani, D. Capriglione & K.Sithamparanathan, “A Practical Demonstration of Spectrum Sensing for WiMAX Based on Cyclostationary Features”, *Foundation of Cognitive Radio Systems, Prof. Samuel Cheng (Ed.), ISBN: 978-953-51-0268-7, InTechOpen 2012.*

[16] Yang Qu, Xue Li , Ruolin Zhou , Chakravarthy, V. , Zhiqiang Wu, “Software-Defined Radio Based Automatic Blind Hierarchical Modulation Detector via Second-Order Cyclostationary Analysis and Fourth-Order Cumulant” , *2013 IEEE Military Communications Conference*

[17] Badawy, A.; Khattab, T. "A novel peak search & save cyclostationary feature detection algorithm", *IEEE Wireless Communications and Networking Conference (WCNC), 2014*

[18] T. Xu, H. Chen and H. Hu, “A Low-Complexity Detection Method for Statistical Signals in OFDM Systems”, *IEEE Communications Letters, Vol. 18, No. 4, April 2014*

[19] Aziz, B. and Nafkha, A, “Implementation of blind cyclostationary feature detector for cognitive radios using USRP”, *2014 21st International Conference on Telecommunications (ICT)*

[20] A. Nafkha, M. Naoues, K.Cichon, A.Kliks, “Experimental Spectrum Sensing Measurements using USRP Software Radio Platform and GNU-Radio”, *DOI 10.4108/icst.crowncom.2014.255415. CROWNCOM 2014, June 02-04, Oulu, Finland*

[21] Martian, A. Sandu, B.T. ; Fratu, O. ; Marghescu, I. ; Craciunescu, R. , “Spectrum sensing based on spectral correlation for cognitive radio systems”, *4th International conference on Wireless Communications, Vehicular Technology, Information Theory and Aerospace & Electronics Systems (VITAE), 2014*

[22] Ettus Research LLC, USRP2, The Next Generation of Software Radio Systems, http://www.ettus.com/downloads/ettus_ds_usrp2_v5.pdf.

[23] W.M. Jang, “Blind Cyclostationary Spectrum Sensing in Cognitive Radios”, *IEEE Communications Letters, Vol. 18, No.3, March 2014*

[24] Ananthram Swami, Senior Member, IEEE, and Brian M. Sadler, Member, IEEE, “Hierarchical Digital Modulation Classification Using Cumulants”, *IEEE Transactions On Communications, Vol. 48, No. 3 March 2000.*

[25] Jerry M. Mendel, Fellow IEEE, “Tutorial on Higher-Order Statistics (Spectra) in Signal Processing and System Theory: Theoretical Results and Some Applications”, *Proceedings of the IEEE, Vol. 79, No. 3 March 1991*

[26] M.Narendar , A. Kumar Krishna , A. P. Vinod , A.S. Madhukumar, “Robust Two-Stage Spectrum Sensing and Policy Management for Cognitive Radios Using Fourth Order Cumulants”, *International Journal Of Information Engineering IJIE Vol. 3, Iss. 2, Jun. 2013, PP. 45-55 www.vkingpub.com © 2011-2012 American V-King Scientific Publishing*

[27] Yang Qu, Xue Li, Ruolin Zhou, Vasu Chakravarthy and Zhiqiang Wu, “Software-Defined Radio based Automatic BlindHierarchical Modulation Detector via Second-OrderCyclostationary Analysis and Fourth-OrderCumulant”, *2013 IEEE Military Communications Conference*

[28] LI Pei-hua, ZHANG Hong-xin, WANG Xu-ying, XU Nan, XU Yuan-yuan, “Modulation recognition of communication signals based on high order cumulants and support vector machine”, *The Journal of China Universities of Posts and Telecommunications, ELSEVIER, June 2012*

[29] Yingpei Lin, Chen He, Lingge Jiang and Di He, “A Spectrum Sensing Method in Cognitive Radio Based on the Third Order Cyclic Cumulant”, *International Conference on Wireless Communications & Signal Processing (WCSP) 2009.*

[30] Liu Liangkaia, Cheng Jian, Li Yongtao, Liu Tao, “Estimation of BPSK Carrier Frequency Based on the High-Order Cyclic Cumulants”, *2011 International Conference on Computer Science and Information Technology (ICCSIT 2011), IPCSIT vol. 51 (2012) © (2012) IACSIT Press, Singapore*

[31] J.P.Lang, “GNU Radio”,Redmine Group, vol. 48,2006-2011

[32] Richard K. Martin, Ryan W. Thomas, and Zhiqiang Wu, "Using Spectral Correlation For Non-cooperative RSS-based Positioning," *Proc. of IEEE SSP, June 2011*.

[33] L. L. H.C. Wu, Senior Member, IEEE, and S. S. Iyengar, Fellow, IEEE, “A Novel Robust Detection Algorithm for Spectrum Sensing”, *IEEE Journal On Selected Areas In Communications, Vol. 29, No. 2, February 2011*

[34] Jaekwon Lee, “Blind Spectrum Sensing Techniques for Cognitive Radio System”, *International Journal of Multimedia and Ubiquitous Engineering, Vol. 3, No. 2, April, 2008*

[35] Shen Da, Gan Xiaoying, Chen Hsiao-Hwa, Qian Liang, Xu Miao, “Significant Cycle Frequency based Feature Detection for Cognitive Radio Systems” , *Proc. of the 4th International Conference on CROWNCOM 2009*

[36] X. Li, Q. Han, Z. Liu and Z. Wu, “Novel Modulation Detection Scheme for Underwater Acoustic Communication Signal Through Short-Time Detailed Cyclostationary Features”, *IEEE GlobeCom, 2013*

[37] J. Lunden and V. Koivunen, “Spectrum sensing in cognitive radios based on multiple cyclic frequencies”, *Proc. 2nd Int. Conf. Cognitive Radio Oriented Wireless Netw. Commun. (CrownCom), pp. 37–43, Orlando, FL, USA, July 31–August 3, 2007*

[38] K. Sithamparanathan and A. Giorgetti, “Cognitive Radio Techniques: Spectrum Sensing, Interference Mitigation, and Localization”, Artech House, Sep. 2012, chapter 3: Introduction to Spectrum Sensing Techniques, [WWW], Available: http://www.artechhouse.com/static/sample/Sith-203_CH03.pdf

[39] X. Liu, Q. Zhang, X. Yan, Z. Feng, J. Liu, Y. Zhu, J. Zhang, “A Feature Detector Based on Compressed Sensing and Wavelet Transform for Wideband Cognitive Radio”, *2013 IEEE 24th International Symposium on Personal, Indoor and Mobile Radio Communications: Mobile and Wireless Networks*

[40] Sajjad A Ghauri, I. M. Qureshi, I. Shah & N. Khan, “Modulation Classification using Cyclostationary Features on Fading Channels”, *Research Journal of Applied Sciences, Engineering and Technology 7(24): 5331-5339, 2014 ISSN: 2040-7459; e-ISSN: 2040-7467 © Maxwell Scientific Organization, 2014*

[41] A.Napolitano, “Cyclostationary Signal Processing and its Generalizations”, *IEEE Statistical Signal Processing Workshop, June 29, 2014*

[42] F. Dimic, G. Baldini and S Kandeepan, 'Experimental detection of mobile satellite transmissions with cyclostationary features', *International Journal of Satellite Communications and Networking, Wiley Publication, April 2014*

[43] J. Norris, B. Taylor, and W. Tyler, “Methods of Detection of Bandlimited Signals on UHF MILSATCOM Downlinks”, *2013 IEEE Military Communications Conference*

[44] Z. Wu, T. C. Yang, Z. Liu & V. Chakarvarthy, "Modulation Detection of Underwater Acoustic Communication Signals Through Cyclostationary Analysis", *IEEE Military Communications Conference, 2012 - Milcom 2012*

[45] G. Fuentes, L. Barbe, K.V. Moer, W. Björsell N., ” Discriminant Analysis for Automatic Signal Detection in Measured Power Spectra. ”, *IEEE Transactions on Instrumentation and Measurement, 2013*